PERFORMANCE OF A CRANKCASE-SCAVENGED TWO-STROKE ENGINE

by

James Richard Wynne

B.S.M.E. University of Florida

1951

SUBMITTED IN PARTIAL FULFILLMENT OF THE

REQUIREMENTS FOR THE DEGREE OF

MASTER OF SCIENCE

AT THE

MASSACHUSETTS INSTITUTE OF TECHNOLOGY

1953

Signature of Author.

Department of Mechanical Engineering

Certified by . . . .

Thesis Supervisor

. . . .

Chairman, Departmental Committee on Graduate Students

ABSTRACT

PERFORMANCE OF A CRANKCASE-SCAVENGED TWO-STROKE ENGINE

by

James Richard Wynne

Submitted to the Department of Mechanical Engineering on January 19, 1953 in partial fulfillment of the requirements for the degree of Master of Science.

An investigation of the effect of altitude on power output of a crankcase-scavenged engine and a study of the crankcase inlet system is described. The relation of the crankcase volumetric efficiency to the scavenging ratio and scavenging efficiency is discussed. Steady flow tests of the crankcase inlet system, which is controlled by reed valves, were made and the results correlated with the volumetric efficiency of the crankcase by means of a Mach Index.

Brake power output was found to vary linearly with inlet density at a rate similar to that of a four-stroke engine. It was noted that the volumetric efficiency of the crankcase determines the scavenging ratio and that this ratio is independent of inlet pressure, provided inlet and exhaust pressures are equal. The relation of the Mach Index to volumetric efficiency was found to be very similar to that of a four-stroke engine, having a critical value beyond which the volumetric efficiency decreased rapidly.

THESIS SUPERVISOR: A. R. Rogowski

TITLE: Associate Professor of Mechanical Engineering

Cambridge 39, Massachusetts
January 19, 1953

Dr. E. B. Millard
Secretary of the Faculty
Massachusetts Institute of Technology
Cambridge 39, Massachusetts

Dear Sir:

In partial fulfillment of the requirements for the Degree of Master of Science at the Massachusetts Institute of Technology, I respectfully submit herewith a thesis entitled, "Performance of a Crankcase-scavenged Two-stroke Engine".

Very truly yours,

James R. Wynne

ACKNOWLEDGEMENT

The author is indebted to Kiekhaefer Aeromarine Motors, Inc., and particularly to Mr. Charles D. Strang for making available the engine for the test program and for the whole-hearted cooperation received throughout.

The author is indeed grateful to Professor A. R. Rogowski for his patient guidance and encouragement and very valuable advice throughout the thesis work. The help and suggestions received from Professor C. F. Taylor, Professor William Leary and Mr. J. Livengood were also most valuable, as was the practical assistance of Mr. D. Doremus and Mr. J. Calloggero.

TABLE OF CONTENTS

INDEX OF FIGURES

LIST OF SYMBOLS

A_p	Piston area, sq. in.
A_v	Reed valve port area, sq. in.
bmep	Brake mean effective pressure, psi
btc	Ignition, degrees before top center
bsfc	Brake specific fuel consumption, lb/bhp hr.
C	Flow coefficient of inlet valves and ports
c_{si}	Speed of sound in inlet air, ft/sec
D_o	Air orifice diameter, in.
E_c	Lower heat of combustion of fuel, Btu/lb.
e_{vc}	Volumetric efficiency of crankcase
e_s	Scavenging efficiency
F_A	Fuel-air ratio, $\dot{M}_f/\dot{M}_a$
fmep	Friction mean effective pressure, psi
g	Acceleration of gravity, ft/sec^2
h_f	Dynamometer load when firing, in.Hg.
h_m	Dynamometer load when motoring, in.Hg.
imep	Indicated mean effective pressure, psi
$\dot{M}_a$	Mass flow of air, lb/sec.
$\dot{M}_f$	Mass flow of fuel, lb/sec.
m	Molecular weight of a gas
N	Engine rotational speed, rpm

p_e	Exhaust tank pressure, in.Hg.abs.
p_i	Inlet tank pressure, in.Hg.abs.
p_o	Static upstream orifice pressure, in.Hg.abs.
R	Universal gas constant
R_s	Scavenging ratio
r	Compression ratio
s	Mean piston speed, ft/min.
T	Absolute temperature, degrees Rankine
t_i	Inlet tank temperature, degrees F
t_o	Upstream orifice temperature, degrees F
t_{plug}	Spark plug gasket temperature, degrees F
V_d	Piston displacement volume, cu.in.
Δh	Pressure differential across air orifice, in. H_2O
Δp_{reed}	Pressure differential across reed valve, in. H_2O
ρ_i	Density of inlet air, lb/cu.ft.
ρ_s	Scavenging density based on inlet temperature and exhaust pressure, lb/cu.ft.
η_o	Ideal indicated efficiency from "fuel-air" cycle
η_i	Actual indicated thermal efficiency of the engine cylinder
η_m	Mechanical Efficiency

I SUMMARY

Tests were made on a crankcase-scavenged two-stroke engine designed for use in a target aircraft to determine the effect of altitude on power output. The speed range of 3500 to 4500 rpm at altitudes up to 24,000 ft. was investigated. In addition, a study was made of the inlet process to the crankcase and its relation to scavenging ratio and scavenging efficiency. Steady flow tests were made of the crankcase inlet system which consisted of reed valves. A modified Mach Index, sometimes called the "gulp factor" was computed for the inlet system in a manner similar to that for a four-stroke engine.

It was found that the brake power output varied linearly with the inlet air density at a rate similar to that of a four-stroke engine. It was noted that the volumetric efficiency of the crankcase determines the scavenging ratio, while the scavenging efficiency is a function of cylinder geometry. The scavenging ratio was found to be independent of inlet pressure where inlet and exhaust pressures are equal. Values of gulp factor in excess of 0.45, which corresponds to 4000 rpm, appear to be accompanied by a rapid loss in volumetric efficiency, although the speed range investigated was not wide enough to be conclusive in this respect.

II INTRODUCTION

The crankcase-scavenged, two-stroke engine offers a simple and relatively cheap form of prime mover capable of high output in comparison to its weight. However, development of two-stroke engines in general and the crankcase-scavenged type in particular, has lagged far behind the four-stroke cycle. In this country, the only significant development work carried on has been in the outboard motor industry and most of this by the trial and error method. For these reasons, a general study of factors affecting the performance of the crankcase-scavenged engine is desirable.

The inherent simplicity of the crankcase-scavenged engine is derived from the use of the up-stroke of the piston to induct a fuel-air mixture into the crankcase. It is then compressed on the down-stroke and admitted to the cylinder through a transfer passage and a set of ports uncovered by the piston while the exhaust takes place through another set of ports. Thus the need for a scavenging blower or complicated valve gear is eliminated, the only requirement being a valve to control the admission of air to the crankcase. This may be of the automatic type or mechanically operated.

Because of the high specific output, the two-stroke engine appears promising for use in small aircraft. The particular engine under test in this thesis was designed for a remotely-controlled target aircraft. The effect of altitude on the performance of the crankcase-scavenged engine is therefore of interest, since there is no evidence of any previous investigation of this subject.

It is seen that the inlet process to the crankcase of the engine is the limiting factor on the air consumption of the engine and is, therefore, worthy of special attention. The process is quite similar to that of a four-stroke engine and the possibility of correlating it with the four-stroke process appears worth investigating, since much more is known about factors which affect the volumetric efficiency of four-stroke engines.

III DESCRIPTION OF APPARATUS

The engine used for these studies was a crankcase-scavenged, spark ignition, two-stroke. It was a four cylinder, V-type air-cooled engine, from which three cylinders had been removed to form a single cylinder test engine. Reed valves controlled the inlet to the crankcase while ports controlled by the piston governed the inlet and exhaust of the cylinder. The specifications of the single cylinder are as follows:

Bore	3.5 in.
Stroke	2.75 in.
Compression ratio	10
Piston displacement	26.5 cu. in.
Piston area	9.62 sq. in.
Total Reed valve area	4.42 sq. in.
Cylinder port timing:	
Inlet open	64 b.b.c.
close	64 a.b.c.
Exhaust open	74 b.b.c.
close	74 a.b.c.

A schematic diagram of the engine and porting arrangement is shown in figure 1.

The engine was mounted on a standard test bed from which a CFR engine had been removed and was coupled to a Star D.C., dynamometer. A roller chain coupling was initially used but this proved unable to withstand the torsional vibration of single cylinder operation. A "Fasts" coupling, which consists essentially of two splined hubs joined by a sleeve with internal mating splines, was substituted. It was decided that the small flywheel on the engine was insignificant compared to the dynamometer armature and it was omitted when the new coupling was installed. This arrangement, which may be seen in figures 2 and 3, proved entirely satisfactory. To aid speed determination, the periphery of the coupling was painted with 36 stripes. When illuminated with a 60 cycle stroboscope, the wheel appears stationary at each hundred rpm.

In order to incorporate an ignition indicator, the engine's magneto was removed and the standard CFR type of ignition substituted. This device uses 110 volts D.C. with the spark occurring on the make, rather than the break, of the contact points. This provides more positive control and better reproducibility, since a time lag of varying duration occurs before a spark is produced by the opening of a set of contacts. The wiring diagram is shown in figure 5. The device may be seen in the photograph, figure 3, and consists of a disk of insulating plastic fastened to the end of the crankshaft and rotating within the circle of a protractor fastened to the engine. A small neon tube set behind a radial slit in the disk produces a luminous line when activated by the ignition circuit and the point at which ignition occurs may be read from the protractor. The plate carrying the contact points is ball bearing mounted on a stub shaft on the end of the crankshaft and is rotated to adjust the ignition timing.

Two stroke engines are known to be extremely sensitive to dynamic effects in the inlet and exhaust systems. For this reason, inlet and exhaust surge tanks having a volume of approximately fifty times the cylinder volume were mounted as close to the engine as possible. These may be seen in the photographs, figures 2, 3, and 4, and a schematic diagram of the air and exhaust flow system is shown in figure 6.

Air was delivered through a standard ASME square-edged orifice meter in a two-inch line from either the atmosphere or the laboratory supercharge system. A throttle valve was provided at the entrance of the inlet tank and pressure and temperature of the inlet air measured in the tank. The connection from the tank to the engine was by means of a short duct having an area of approximately four times that of the inlet port and a short 45 degree elbow connecting the duct to the air inlet flange on the engine.

The exhaust tank was designed so that the existing duct on the engine leading from the exhaust ports opened directly into the tank. Construction was sufficiently heavy (3/16 and 1/4 inch steel plate) to provide safety in case of an explosion of unburned mixture in the tanks after motoring the engine; this never occurred, however. In addition to a manometer tap, fittings were provided to cool the tank with a water spray. The exhaust throttle valve in a two-inch line leaving the tank was located high enough to prevent water surging through it. The exhaust line may be connected to the trench for atmospheric exhaust or to the vacuum pump for reducing exhaust pressure.

A cooling blower capable of supplying a maximum duct pressure of 13 in. H_2O was provided. This proved barely adequate to keep the spark plug gasket temperature below the desired 400°F at sea level but cooling requirement decreased rapidly with lower inlet pressures. A field rheostat on the motor driving the blower permitted an adjustment of the duct pressure. The spark plug gasket temperature was measured with an iron-constantan thermocouple and a potentiometer with self-compensating cold junction.

The fuel-oil mixture was supplied to the engine from a 15 gallon tank by an electric motor-driven pump. Fuel pressure was set with the regulator to 10 psi and was controlled after passing through a calibrated rotameter by means of a valve in the line leading to the engine. The existing needle valve on the engine where the fuel is sprayed into the air stream was used as a back-pressure control to prevent vaporization of fuel in the lines. The fuel flow system is shown in figure 7.

Shortly after beginning altitude testing, it became apparent that significant air leakage was occurring into the crankcase. (see Appendix G for discussion). To correct this, new seals were installed at the front and rear of the crankshaft and all other openings in the crankcase were carefully sealed. Two Garlock Klozures, which are a heavy-duty type of seal, were installed back-to-back at the front of the engine and one facing outward was placed at the rear of the engine. The position of these seals may be seen in figure 1. This substantially reduced the leakage and a correction factor was determined for the amount remaining.

IV TEST PROCEDURE

Since this engine was designed to operate in the aircraft only at maximum output, it was desired to determine first the performance over the speed range of 3500 to 4500 rpm at altitudes up to 30,000 ft. In all runs except one, the inlet and exhaust pressures were held equal and controlled by throttling the inlet from the atmosphere and throttling the exhaust to the vacuum pump.

Preliminary testing was done to determine best power fuel-air ratio and spark advance. These quantities are known to be essentially constant with respect to inlet pressure and over this speed range the best power spark advance was also practically constant at 37 degrees b.t.c. Due to air leakage into the crankcase, it was necessary to change the observed fuel-air ratio with inlet pressure to keep the true fuel-air ratio at best power. This is discussed in Appendix G. The values of observed fuel-air ratio used were:

p_i	F_A
27.2 in.Hg.abs.	0.079
20.0	0.0835
15.0	0.0835
11.5	0.086

Fuel used for all runs was 100 octane gasoline with 10% SAE 30 uncompounded oil added for lubrication. The fuel-oil mixture was sprayed into the air inlet of the crankcase. Runs were made at speeds of 3500, 4000 and 4500 rpm with inlet (and exhaust) pressures of 27.2, 20.0, 15.0 and 11.5 in.Hg.abs. These pressures correspond to 2500, 10,750, 18,000, and 24,000 ft. altitude respectfully. The pressure of 27.2 in.Hg.abs. was the highest obtainable when operating with atmospheric inlet; it was chosen as the basis for comparison to eliminate the complication of having to operate the supercharge compressor for some runs. The pressure of 11.5 in.Hg.abs. was the lowest obtainable as limited by the capacity of the exhaust vacuum pump. One set of runs was made with the inlet and exhaust pressures at 22 and 20 in.Hg.abs. respectively.

In obtaining a test point, the speed was set by adjustment of the dynamometer field control in conjunction with the tachometer and stroboscope and the inlet and exhaust pressures adjusted to the desired value. The air flow was then determined and the rotameter set to deliver the best power fuel-air ratio for that inlet pressure. The cooling air duct pressure was adjusted to maintain the desired spark plug gasket temperature. Due to the wide variation in cooling requirement with inlet pressure, it was not possible to hold a constant temperature for all runs. The values used were:

p_i	t_{plug}
27.2 in.Hg.abs.	400 °F
20.0	400
15.0	350
11.5	300

When steady conditions were obtained, the dynamometer load and inlet air temperature were recorded. Motoring friction was determined by cutting the ignition without changing the setting of inlet and exhaust throttle valves. In order that friction readings be taken at near-operating temperature, a procedure was evolved whereby the cooling blower was cut first and the plug gasket temperature allowed to increase 50°F. The ignition was then cut and the engine brought up to its original speed by motoring the dynamometer. The friction load was recorded when the plug temperature passed by its previous value as the engine cooled.

Steady flow tests of the reed valves were made by removing the cylinder and connecting the exhaust tank to the opening in the crankcase. The vacuum pump was used to draw air through the inlet system, thus eliminating any effect of pressure fluctuations from a compressor supplying the air flow. The air flow, temperature, pressure drop across the reed valves and the pressure in the inlet and exhaust tanks were recorded when steady conditions were obtained at each test point.

V MECHANICAL FAILURES

Two types of structural failures occurred during the test program. These were unrelated to each other and will be discussed separately.

Reed Valves

Reed valves are thin (.005 - .010 in.) pieces of metal covering the port opening and attached at only one point. A pressure below the reed lower than that upstream causes the reed to bend away from the port and allow a flow to take place. The reed springs closed when the pressure difference is removed and seals against a pressure differential in the opposite direction. A stop of heavier material limits the distance the reed can bend open. In high-speed operation, the frequency of opening and closing is such that the motion becomes effectively a vibration with an impact each time the reed contacts the stop and the port, making an exact stress analysis practically impossible.

The type of reed and stop originally found in the engine are shown in figure 8 marked "old". Six of these reeds were arranged in a circle around the crankshaft to admit the mixture to the crankcase. It may be seen that the shapes are such as to invite the reed to bend sharply at the edge of the stop when contact occurs. This is obviously a point of stress concentration and the photograph shows that the failure initiated at this point. Engine operation became rough and a loss in power and air consumption was noted. The total time to this failure is not known as the engine had been run at the factory before these tests began. The entire set of reeds was replaced and the edges of the stops rounded to lessen the stress concentration at this point. Operation was satisfactory for 15 hours when another reed broke, this time across the entire reed just beyond the point of attachment where the bending stress is greatest. In both cases, the reeds apparently broke up and passed through the engine; no damage was done and no trace found of the reeds.

Analysis at this point indicates two conclusions; (1) the reed stop should be of similar shape to the reed to prevent the bending of the reed around the edge of the stop, (2) the bending stress at the point of attachment must be reduced or a material of higher endurance limit be substituted.

All of these factors were included in new style of valve supplied by the manufacturer at this time and shown in figure 8 ("new"). The shape of the stop is similar to the reed and material is beryllium copper, insteady of steel, which improved the endurance limit. In addition, the reeds were made smaller and the number increased to ten, thereby helping to reduce the stress. Total port area remained approximately the same. Thirty hours running time was accumulated on the new valves with no indication of trouble and the manufacturer reports no reed failures since the change.

Connecting Rod

Figure 8 shows the failure of the connecting rod which occurred after 45 hours running. It was later learned that previous time on the engine amounted to 350 hours, making a total of about 400 hours to failure. Since the design life of the engine in a target aircraft is only about 25 hours, the life of this rod is adequate; however, the design change to extend the endurance life is quite obvious and extremely simple. It may be seen that notches are present both in the rod and the cap where they were spot-faced for the bolt head and nut. The effect of a notch in a part in cyclic loading is well known and this failure is a perfect example of a fatigue crack initiating at the point of stress concentration. Inspection revealed that the crack had progressed approximately half way through the material when the stress became sufficient to rupture the remaining section. The removal of this notch would extend the endurance life of the rod many times.

The engine was operating at 3500 rpm and atmospheric inlet pressure at the time of failure. Damage in addition to the connecting rod included a broken piston and rings, two holes and several cracks in the crankcase, scored cylinder, and scored and apparently bent crankshaft.

It was suggested by the manufacturer that at low inlet pressures the inertia force on the rod may be greater than the gas forces. This would cause a complete reversal of stress in the rod rather than the unidirectional stress generally assumed present in a two-stroke connecting rod. However, an estimate of the forces involved (Appendix F) shows that the inertia force exceeds the gas force at maximum speed even at sea level. Hence this was not a contributing factor to the failure.

VI DISCUSSION AND RESULTS

A tabulation of observed and calculated data is given in Appendix A. A summary of the performance with the old-style reed valves is included therein but the curves summarizing the altitude performance of the engine, figures 11 to 15 inclusive, are with the new-style valves.

The performance runs were made at pressures corresponding to various altitudes but at constant inlet temperature. The method used to correct the data for altitude temperatures is given in Appendix B and it is believed that the results represent a close approximation to the actual performance at altitude. A sample calculation for one test point is shown in Appendix C.

It will be observed that the power output varies linearly with the density. Figure 11 was plotted with the indicated horsepower at the test condition nearest sea level pressure as the reference point. This was then extrapolated to determine the power at sea level pressure and this value used as the base for figure 12 in order that comparison with data from other sources might be made. The rate of change of power with density in figure 12 is quite similar to that given in Taylor and Taylor(1) for several four-stroke engines, indicating that the effect of altitude on power output is almost the same for the crankcase-scavenged as for the four-stroke engine. The three slopes in figure 12 correspond to differing mechanical efficiency at the three speeds. The friction horsepower decreases only slightly with inlet pressure while the power decreases rapidly; hence, the mechanical efficiency at altitude decreases rapidly, since

$$\eta_m = \frac{bhp}{bhp + fhp}$$

The rate of decrease of power output is greatest for the lowest mechanical efficiency (4500 rpm). The effect of altitude on mechanical efficiency is shown in figure 13.

The absolute values of bhp and bsfc at altitude are shown in figure 14. The bsfc was computed using the value of bhp corrected for temperature and a fuel flow rate corrected to keep the same fuel-air ratio with the increased air density. The values of bmep corrected for altitude are plotted in figure 15, together with the fmep observed in the test; fmep is essentially independent of the temperature correction. It will be noted that the fmep decreases slightly with inlet pressure, apparently due to decreased bearing loads.

The points taken with 22 in.Hg.abs. inlet pressure and 20 in.Hg.abs. exhaust pressure simulate the result of boosting the inlet pressure 2 in.Hg. while at an altitude of 10,750 ft. It will be noted that the bsfc for this condition increased markedly since a large quantity of fresh mixture was lost in scavenging. It is generally agreed that supercharging a two-stroke engine is not profitable unless the exhaust pressure is also raised, as with an exhaust turbine. These results substantiate this for the crankcase-scavenged two-stroke.

As defined in Taylor and Taylor[2], the scavenging ratio of a two-stroke engine is the ratio of the weight of mixture pumped to the weight which would fill the entire cylinder volume (at bottom center) at inlet temperature and exhaust pressure. The scavenging efficiency is defined as the ratio of the weight of mixture retained in the cylinder to the weight which would fill the entire cylinder volume at inlet temperature and exhaust pressure. Exhaust pressure is chosen because, due to the late closing of the exhaust ports, the pressure during compression is usually never higher than if the process started at bottom center and exhaust pressure. The scavenging ratio is calculated from the measured air flow supplied to the engine but the amount which is retained in the cylinder is not so easily determined. The method used to estimate the scavenging efficiency is illustrated in Appendix D. Figure 16 shows the variation of scavenging ratio with speed both as observed and corrected for leakage as discussed in Appendix G. Figure 17 shows the variation of scavenging efficiency with scavenging ratio at the various inlet pressures and constant inlet air temperature. The cross-hatched area is the range of values obtained from tests with the M.I.T. two-stroke engine.[3] It should be pointed out that these values represent extensive experimentation with port geometry. The 45° line represents theoretical scavenging with no mixing or short circuiting to the exhaust ports and the other curve represents theoretically perfect mixing of fresh mixture and residual gas. It will be noted that the lower scavenging ratios at each inlet pressure correspond to the higher engine speeds. This is because the scavenging ratio is determined by the volumetric efficiency of the crankcase and over the speed range studied, this value decreased as the speed was increased. The figure shows that a slight drop in scavenging efficiency accompanied a decrease in inlet pressure at a given scavenging ratio. The reason for this is not apparent; one supposition might be that the decrease in Reynolds number with the lower flow rate changed the flow pattern through the cylinder. However, the change was so small as to be insignificant for the purposes of this study.

It has been seen that the volumetric efficiency of the crankcase limits the air capacity of the engine. When the inlet and exhaust pressures are equal, the scavenging ratio can therefore only approach $\frac{r - 1}{r}$ as a limit, r being the compression ratio. The usual definition of volumetric efficiency is the ratio of the weight of mixture pumped to the <u>displaced</u> cylinder volume at inlet density. Hence, where $p_e = p_i$, $R_s = \frac{r-1}{r}(e_{vc})$ and since the limiting value of e_{vc} is 1.0, the limit of R_s is $\frac{r-1}{r}$. The efficiency of the engine as an air pump may therefore be evaluated either in terms of the scavenging ratio or of the volumetric efficiency of the crankcase. Because of its similarity to the four-stroke inlet process, the volumetric efficiency of the crankcase was chosen for examination.

Extensive investigation has yielded a factor for expressing the flow capacity of a four-stroke inlet valve called the "gulp factor".[4] It has been found that engines of varying design all have a critical gulp factor in the vicinity of 0.5, beyond which volumetric efficiency drops rapidly. This is a parameter of extreme importance in four-stroke engines and an attempt was made to apply it to the crankcase inlet process in these tests.

The method of calculation is shown in Appendix E. It will be noted that a quantity, C_{av}, is required in the expression for gulp factor in the four-stroke process. This is a coefficient for steady flow through the valve averaged over the lift curve of the valve. Since the flow coefficient of reed valves is a function of the pressure difference across them, it was assumed that the valve opened and closed instantaneously. The open duration of the valve was taken as 150 degrees of crankangle from information supplied by the manufacturer. These assumptions made possible the determination from the results of steady flow tests, an average flow coefficient roughly corresponding to C_{av}. With this determined, the gulp factor was calculated for the three speeds at the 27.2 in.Hg. inlet pressure condition. The values of crankcase volumetric efficiency of this engine together with the range of several four-stroke engines are plotted against gulp factor in figure 21. This shows that over the narrow speed range evaluated in these tests, the trend of volumetric efficiency is similar to that of the four-stroke engines. If this is true, it is apparent that values of gulp factor in excess of 0.45 result in rapid loss in volumetric efficiency. The number of test points should be increased before a conclusion is drawn, however.

VII CONCLUSIONS

1. The power output of the crankcase-scavenged two-stroke engine decreases linearly with the inlet density at a rate similar to that of a four-stroke engine. The decrease would bring the ratio of bhp/bhp$_{\text{sea level}}$ to zero at an altitude of approximately 40,000 ft.

2. The scavenging ratio is independent of inlet pressure provided inlet and exhaust pressure are equal. e_{vc}

3. Attempting to supercharge by boosting the inlet pressure without regard to the exhaust pressure is uneconomical because of the large loss of fresh mixture during scavenging.

4. The scavenging ratio of the crankcase-scavenged engine is determined by the volumetric efficiency of the crankcase; the scavenging efficiency at a given scavenging ratio is a function of the flow characteristics of the cylinder, piston, and port assembly. The crankcase volumetric efficiency is comparable to that of a four-stroke engine and is a function of the flow capacity of the inlet valves or "gulp factor." Values of gulp factor in excess of 0.45 appear to be accompanied by a rapid loss in volumetric efficiency, although the speed range investigated was not wide enough to be conclusive in this respect.

VIII RECOMMENDATIONS FOR FUTURE RESEARCH

Because of the limited life of this engine, only a narrow speed range was investigated. The extension of these tests to different speeds would be interesting; especially should the information concerning the scavenging ratio and crankcase volumetric efficiency be so extended. A pressure-time diagram for the crankcase would reveal the actual pressure drop across the reed valves and the exact duration of the inlet process, permitting a more accurate determination of the value of the flow coefficient. This, together with a larger number of test points over a wider speed range, would extend the curve of volumetric efficiency vs. gulp factor and check the value of the critical gulp factor.

It would be helpful to have an engine designed for test purposes which would be rugged enough to withstand continuous usage. It should be possible to try various types of valves for controlling the crankcase inlet process, both automatic and mechanically operated, to obtain optimum volumetric efficiency. Arrangement should be made for varying the cylinder port geometry to obtain the best scavenging efficiency possible at a given scavenging ratio. A thermocouple located in the transfer passage would help determine the true conditions of the mixture as it enters the cylinder.

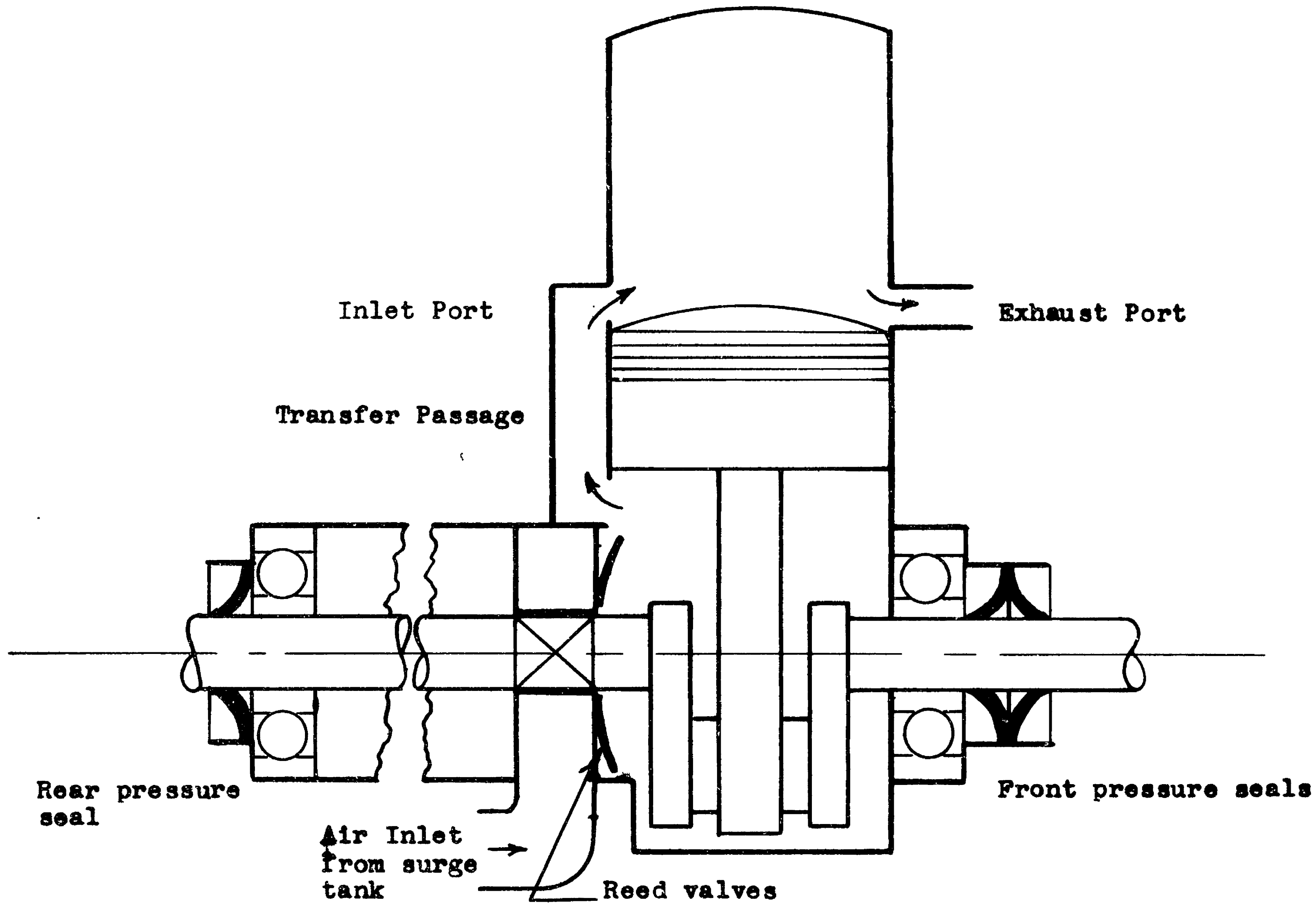

Figure 1

Engine Porting Arrangement

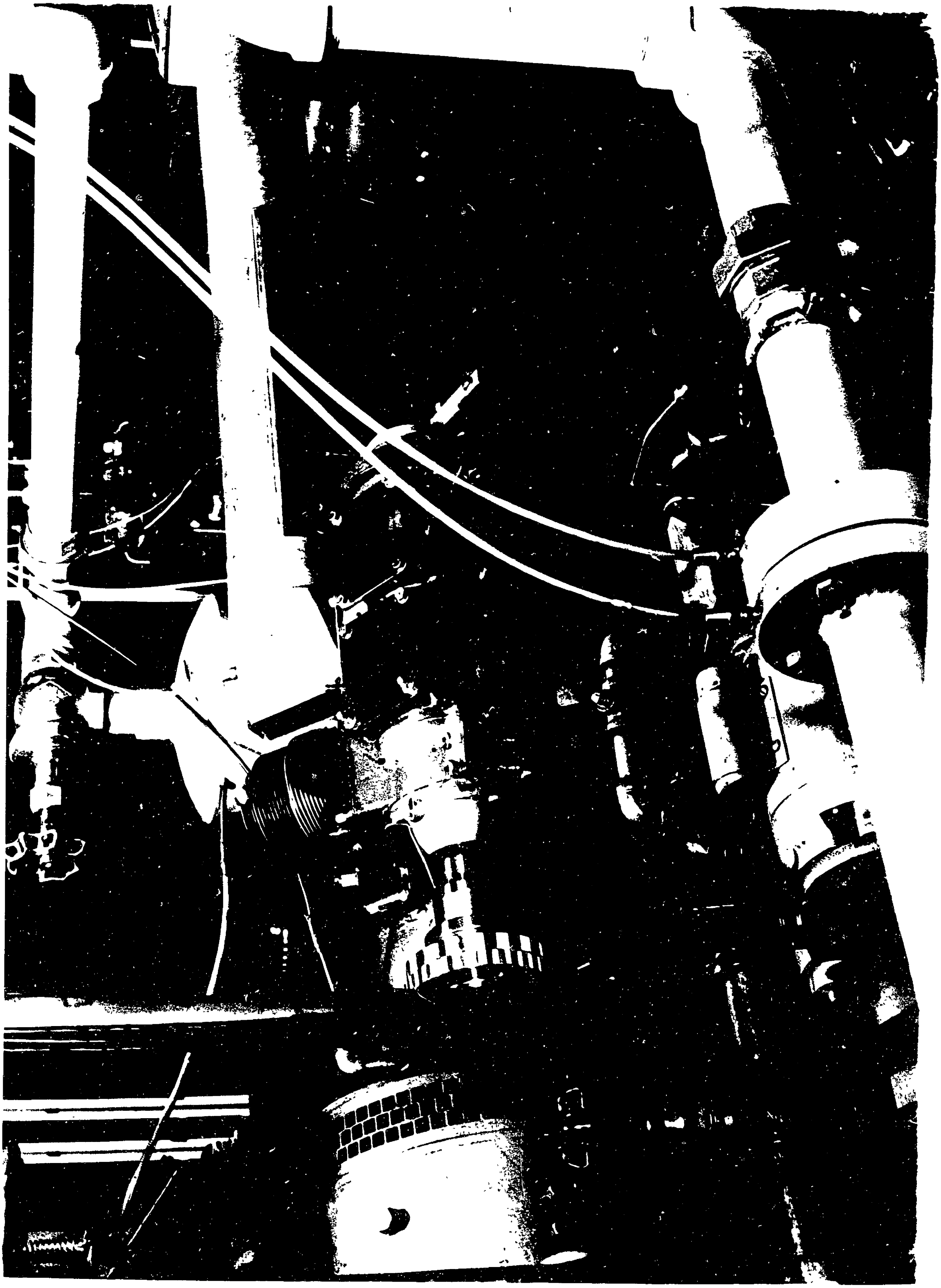

FIGURE 2

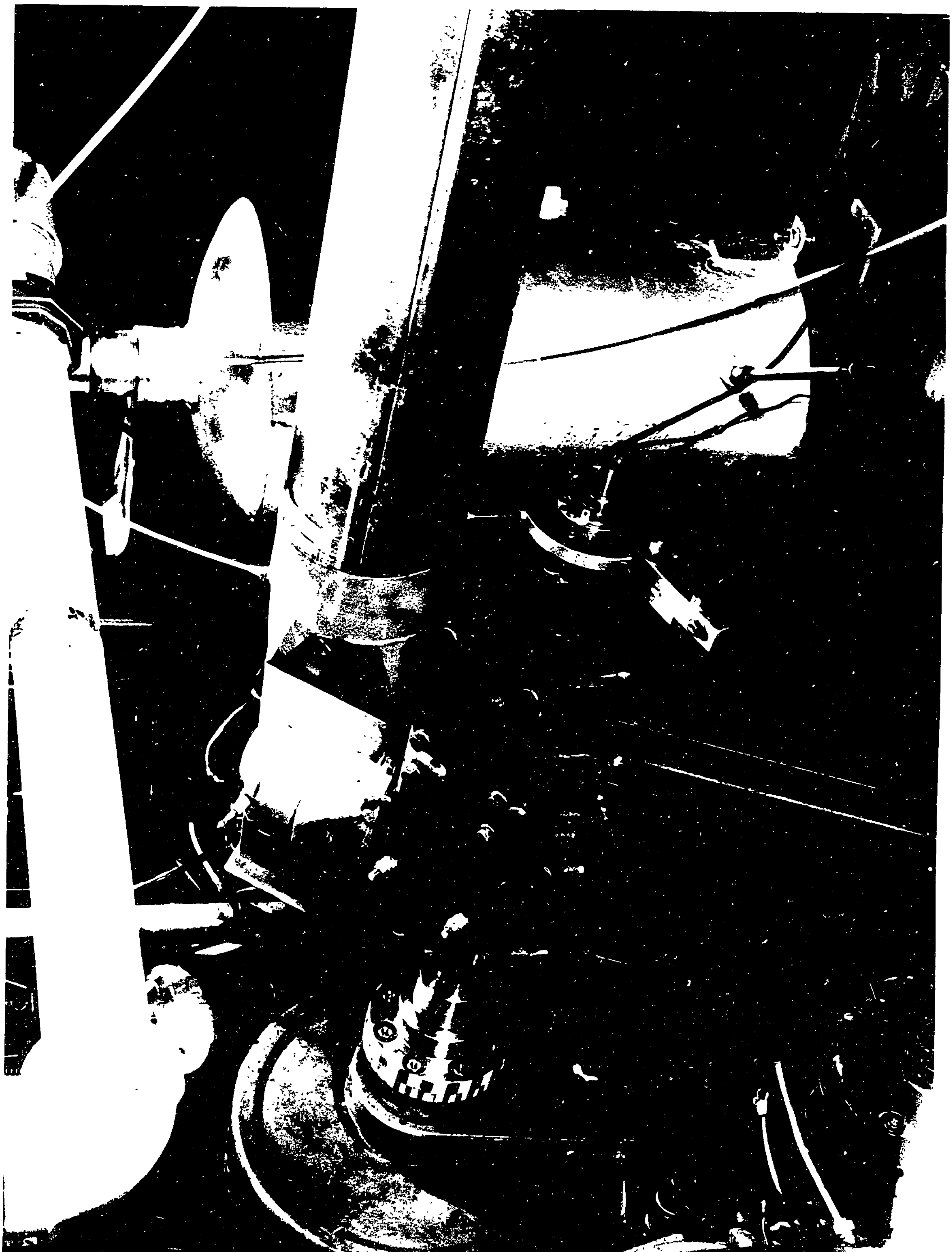

FIGURE 3

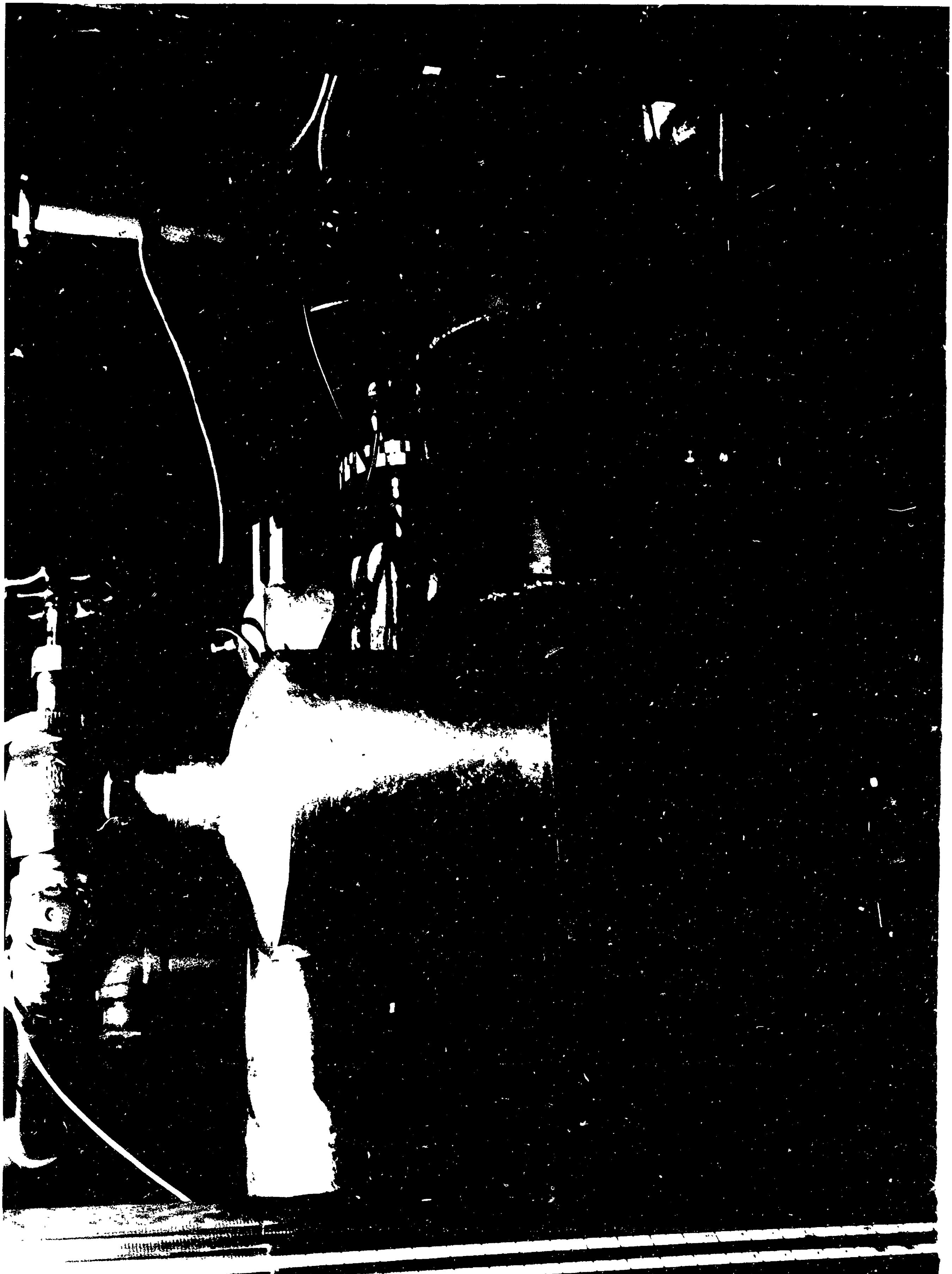

FIGURE 4

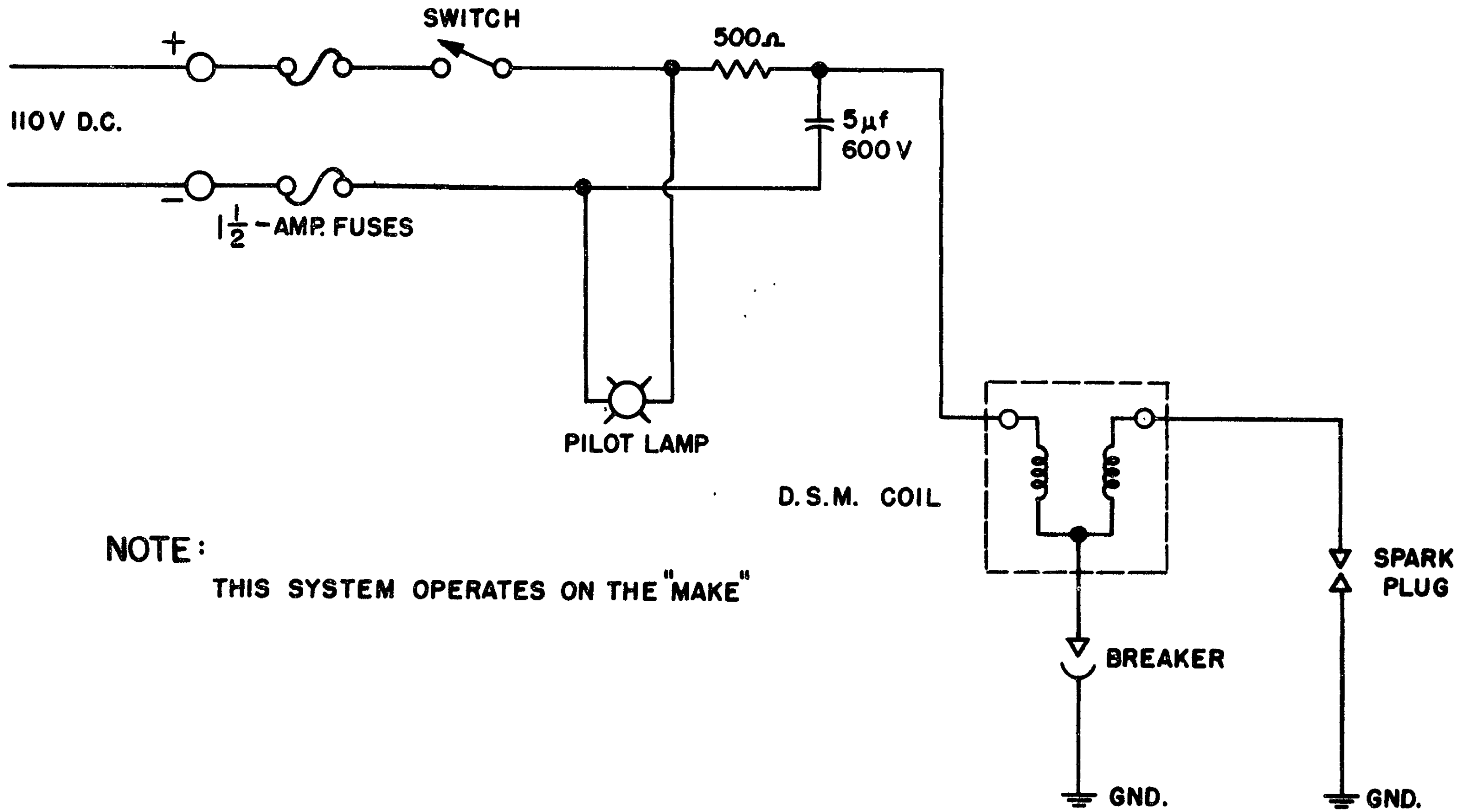

Figure 5

WIRING DIAGRAM OF IGNITION SYSTEM

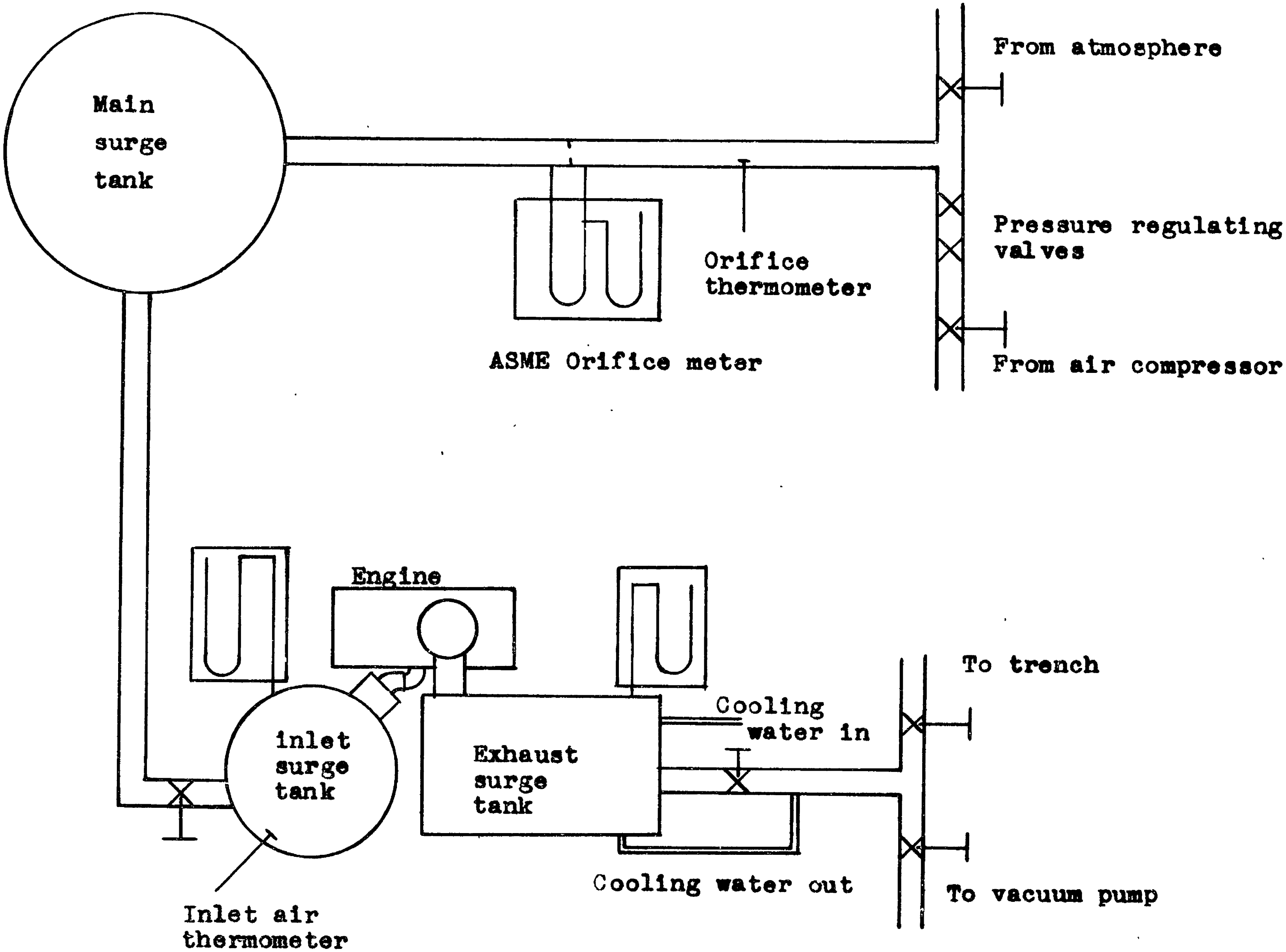

Figure 6

Air and Exhaust Flow System

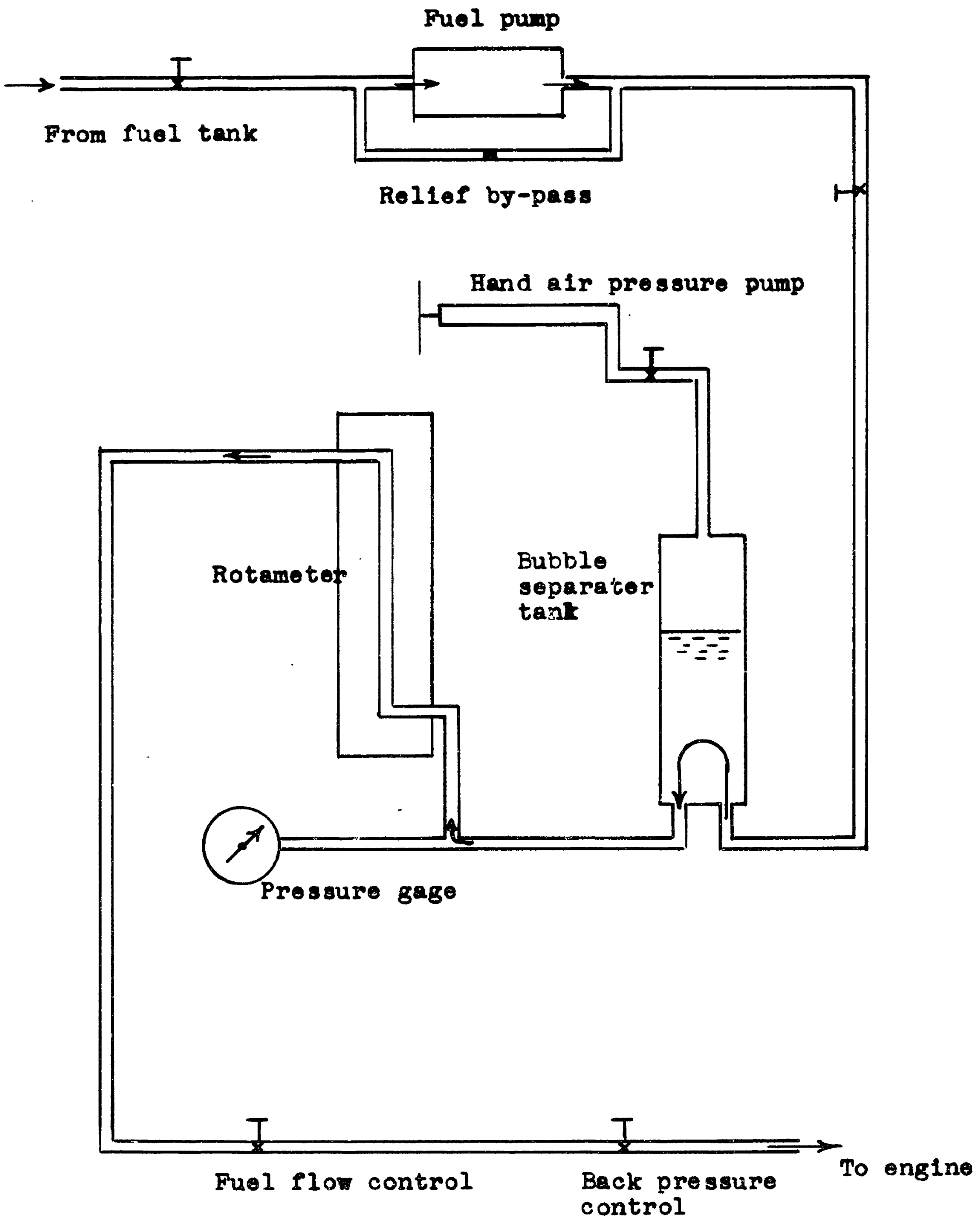

Figure 7

Fuel Flow System

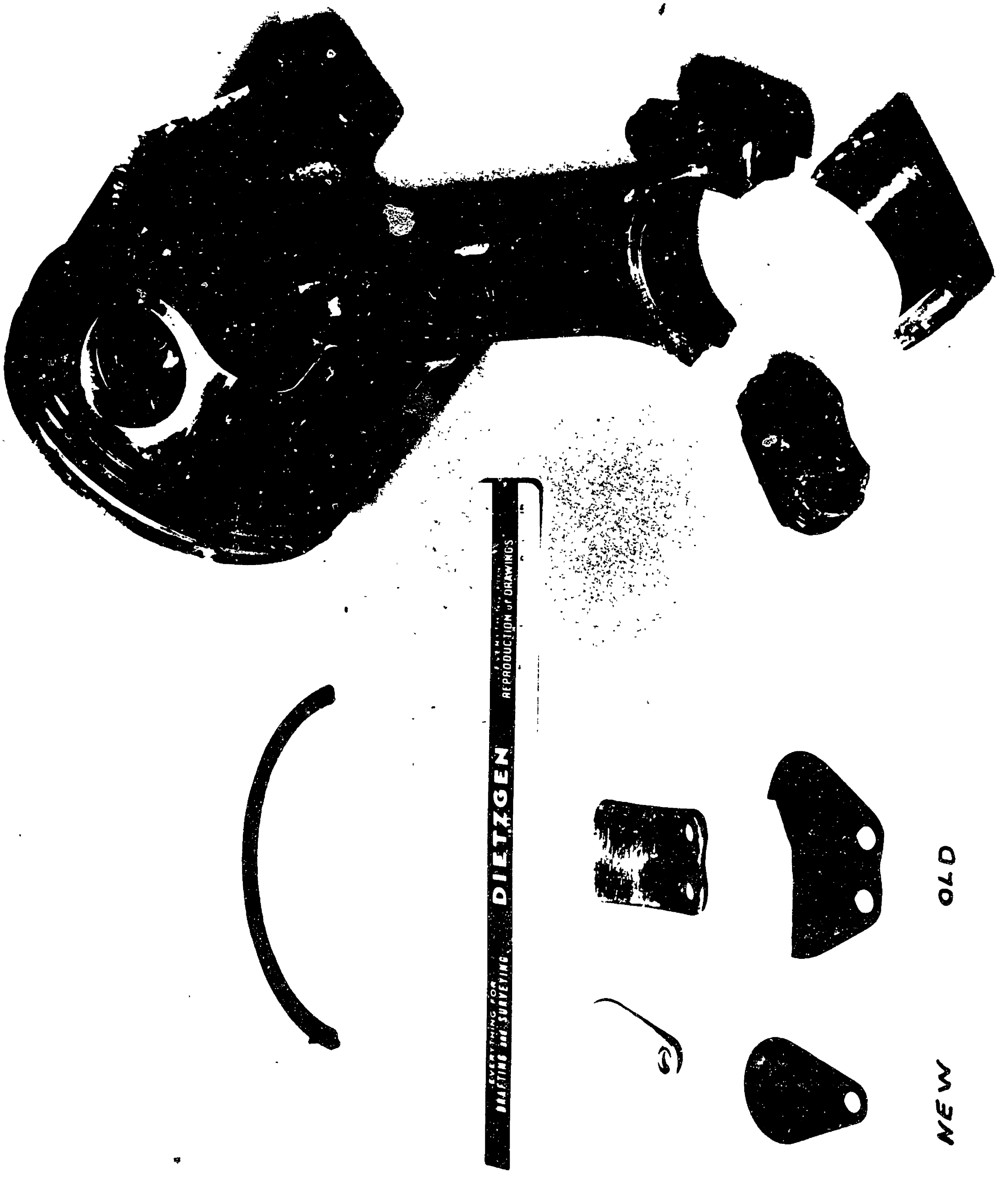
EVERYTHING FOR
DRAFTING AND SURVEYING
DIETZGEN
REPRODUCTION of DRAWINGS
NEW
OLD

FIGURE 8

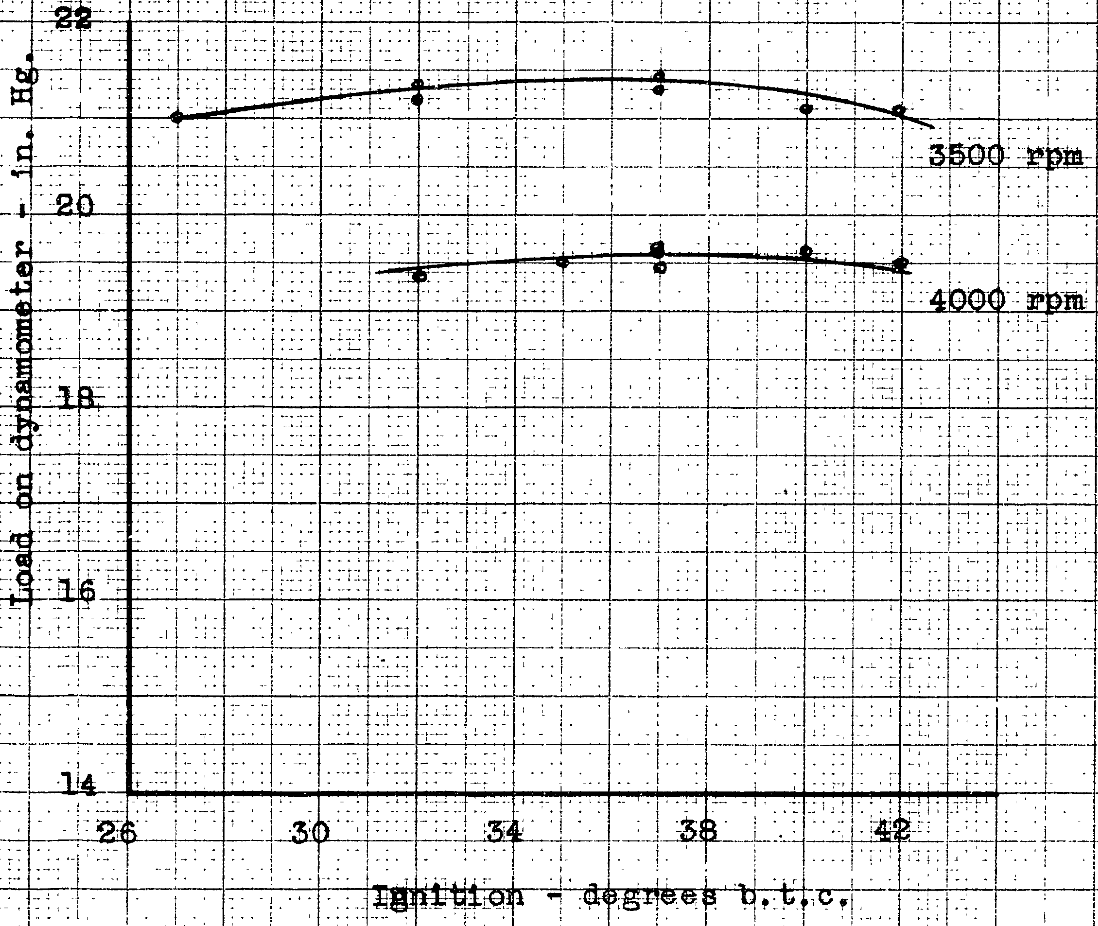

Figure 9

Brake Load vs Spark Advance

$p_e = p_i = 28.0$ in. Hg. abs.

$F_A = 0.078$

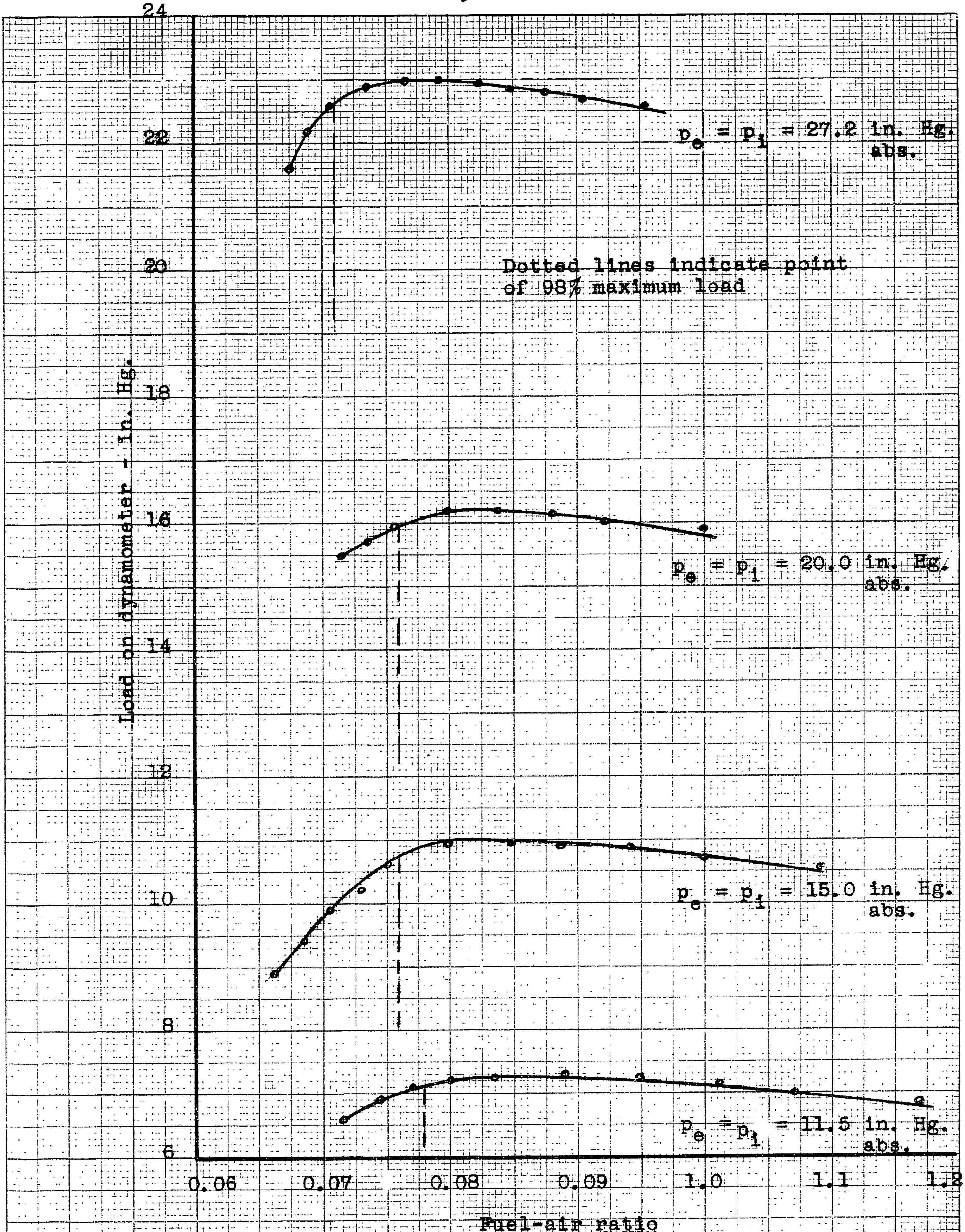

Figure 10 - Load vs Fuel-air Ratio at Several Pressures
Spark = 37 degrees b.t.c. 3500 rpm

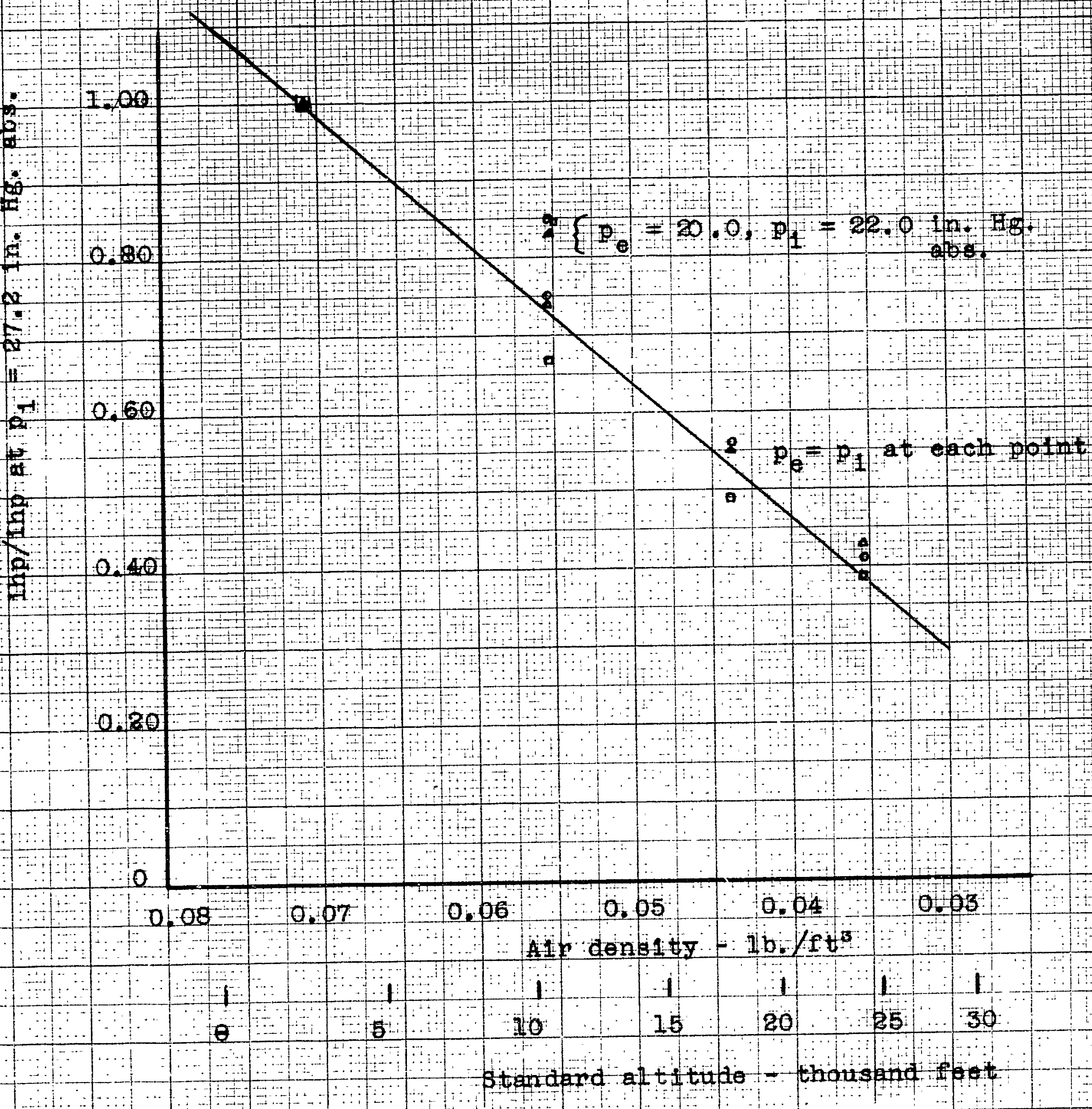

Figure 11

Indicated Horsepower vs Air Density

○ 3500 rpm
△ 4000 rpm
□ 4500 rpm

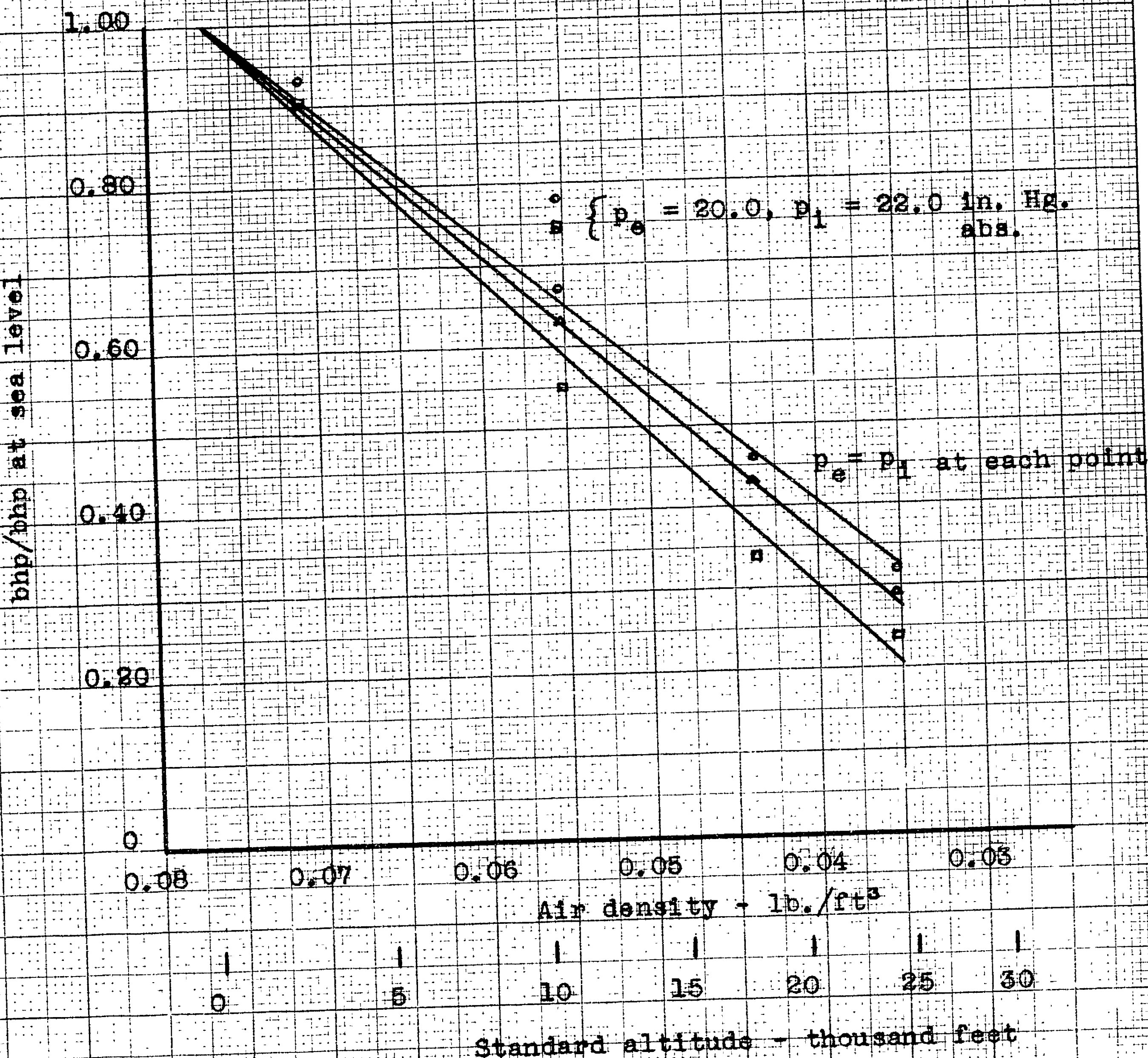

Figure 12

Brake Horsepower vs Air Density

○ 3500 rpm
△ 4000 rpm
□ 4500 rpm

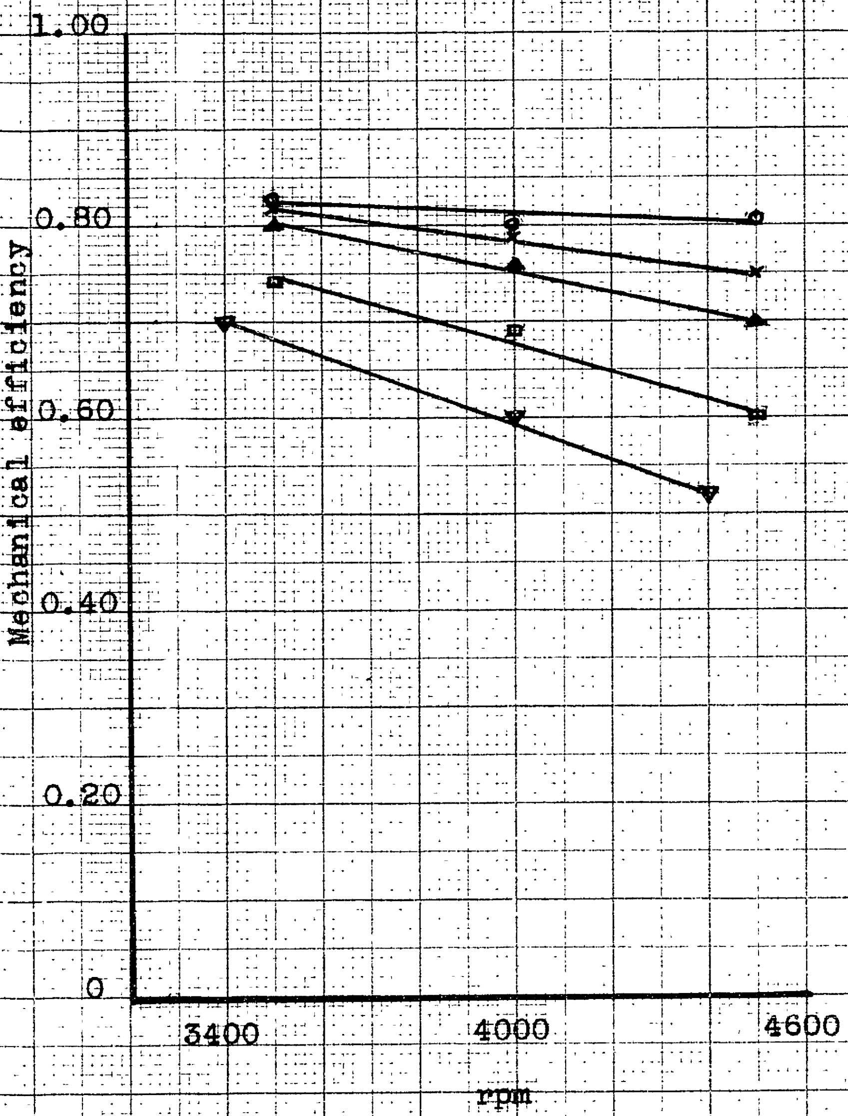

Figure 13 - Effect of Altitude on Mechanical Efficiency

▼ $p_e = p_i$ = 11.5 in. Hg. abs.

□ $p_e = p_i$ = 15.0

△ $p_e = p_i$ = 20.0

○ $p_e = p_i$ = 27.2 in. Hg. abs.

× p_e = 20.0, p_i = 22.0 in. Hg. abs.

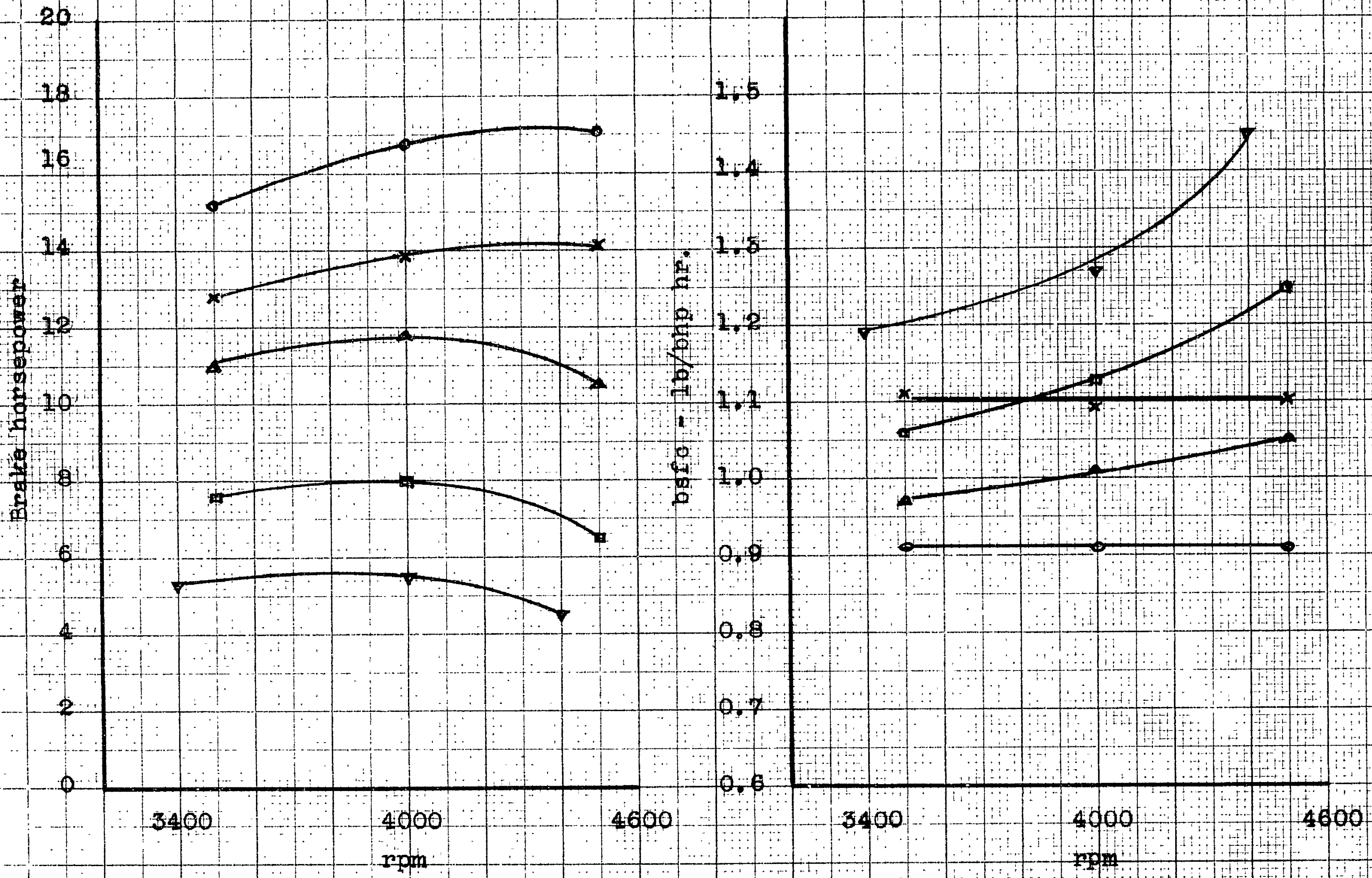

Figure 14
Brake Horsepower and Brake Specific Fuel Consumption at Altitude
Symbols given in Figure 13

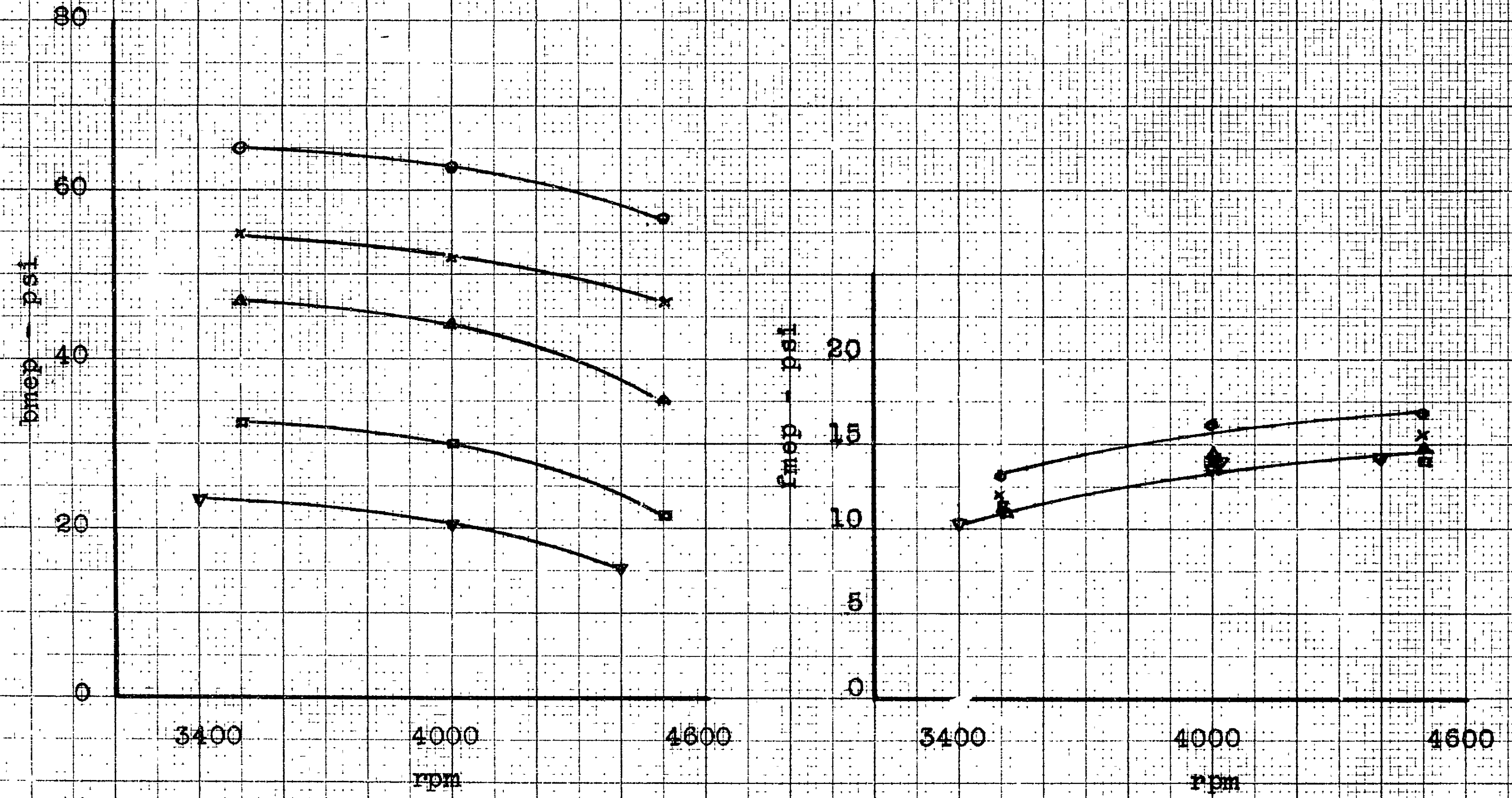

Figure 15
Brake mean effective pressure and friction mean effective pressure at altitude
Symbols given in Figure 13

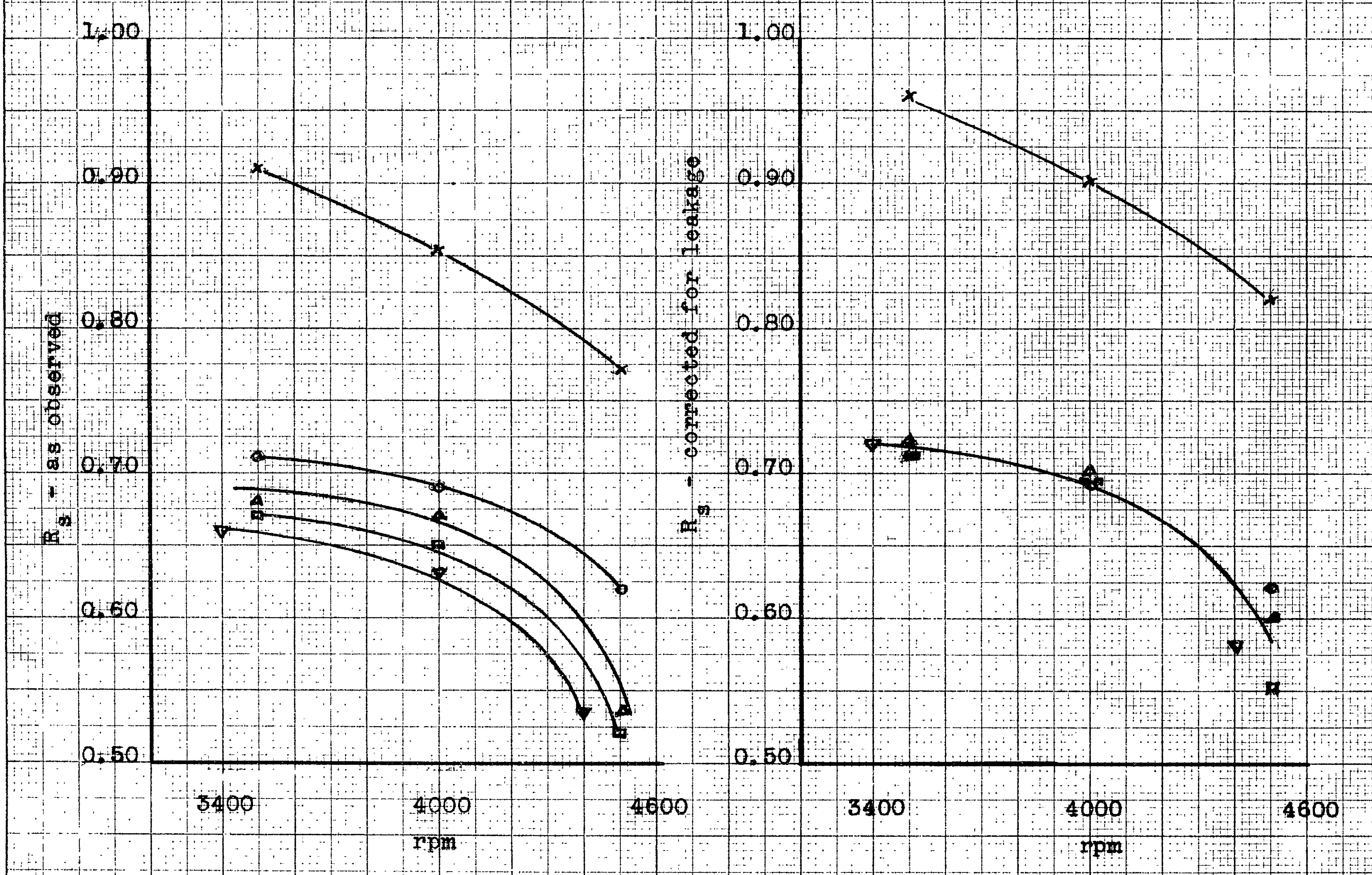

Figure 16
Scavenging Ratio (uncorrected and corrected) vs Speed at Several Pressures
Symbols given in Figure 13

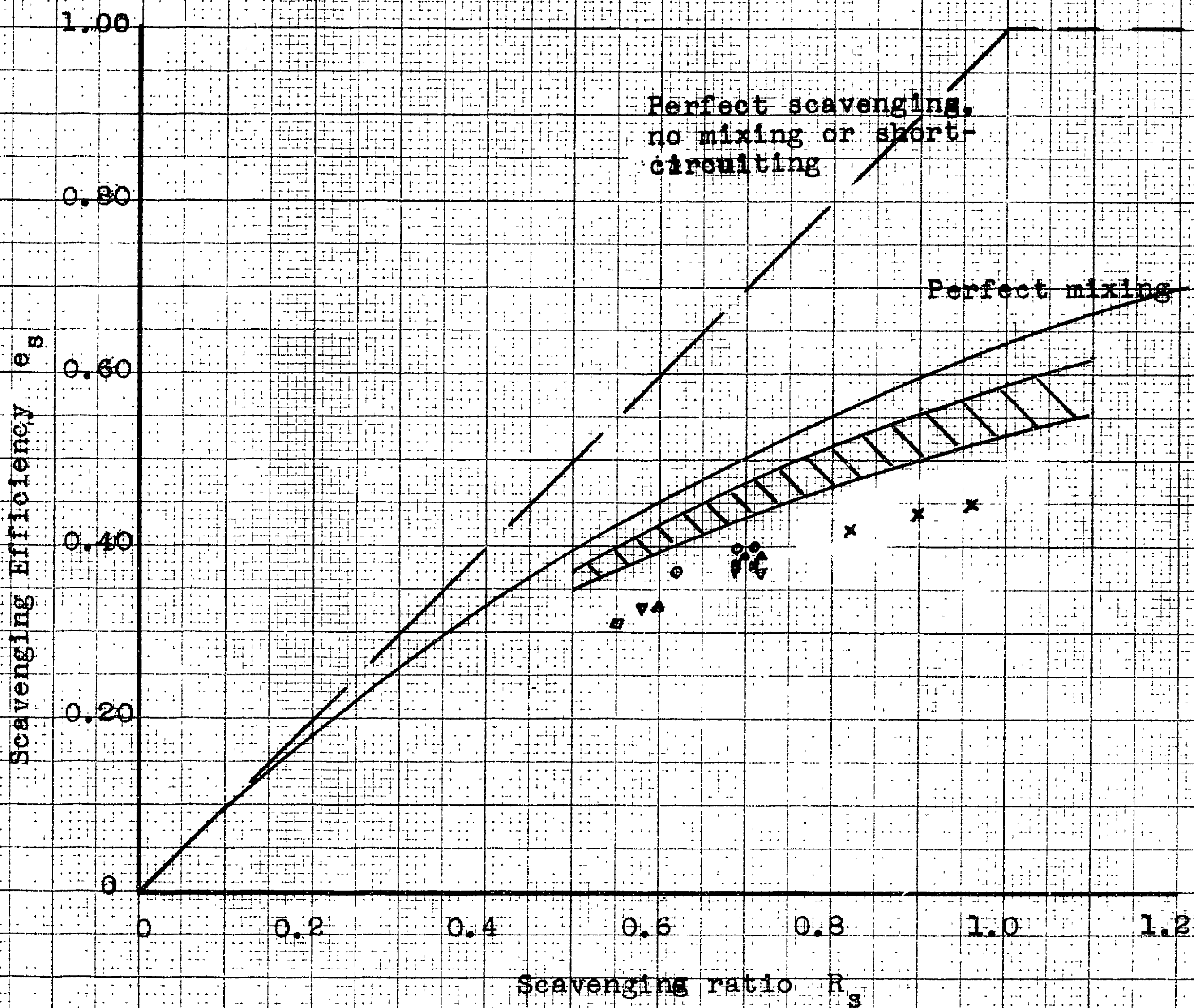

Figure 17

Scavenging Ratio vs Scavenging Efficiency

Cross-hatched area denotes range of values obtained with the M.I.T. Two-stroke Engine

Symbols given in Figure 13

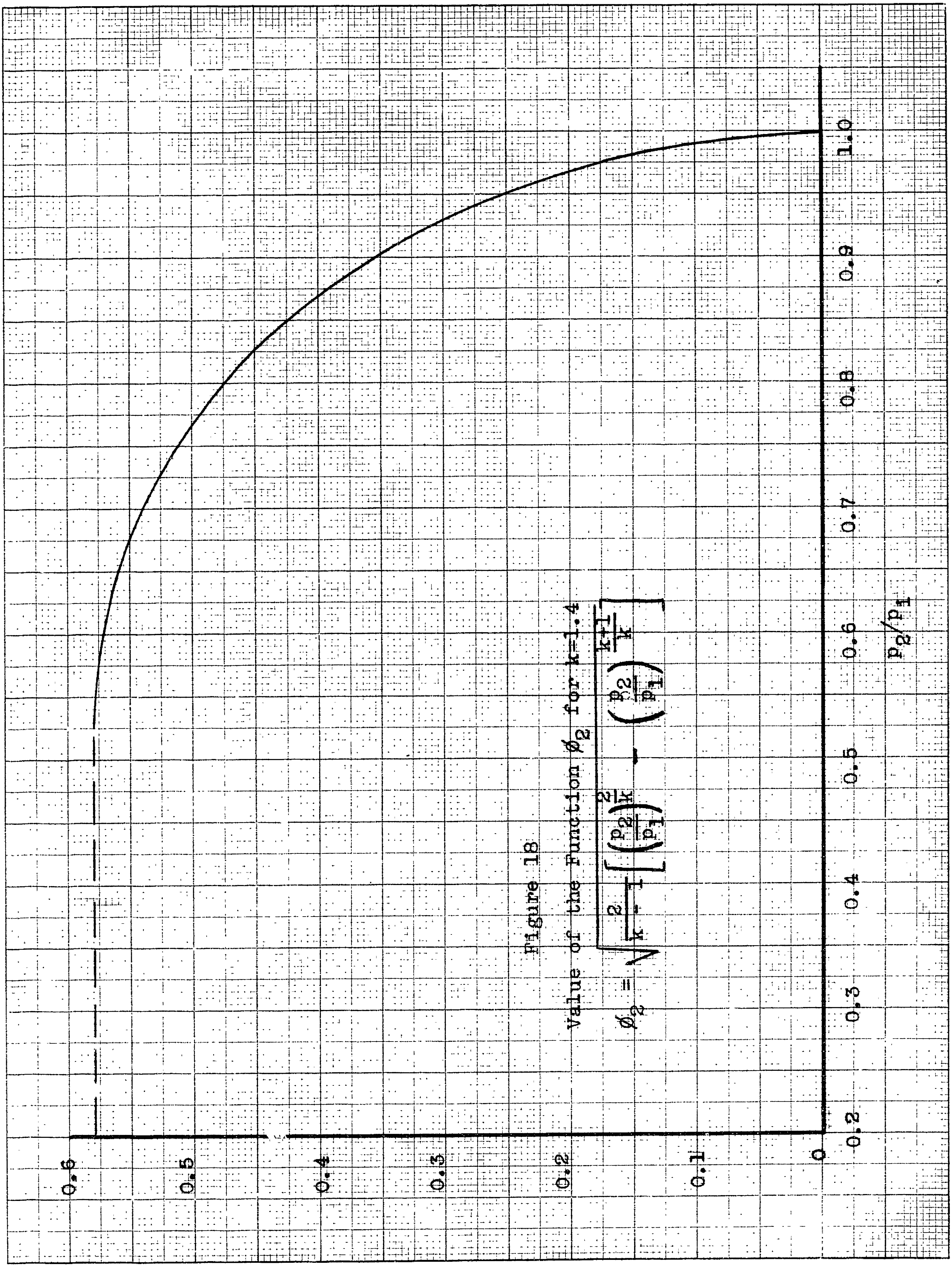

Figure 18

Value of the Function ϕ_2 for k=1.4

$$\phi_2 = \sqrt{\frac{2}{k-1}\left[\left(\frac{p_2}{p_1}\right)^{\frac{2}{k}} - \left(\frac{p_2}{p_1}\right)^{\frac{k+1}{k}}\right]}$$

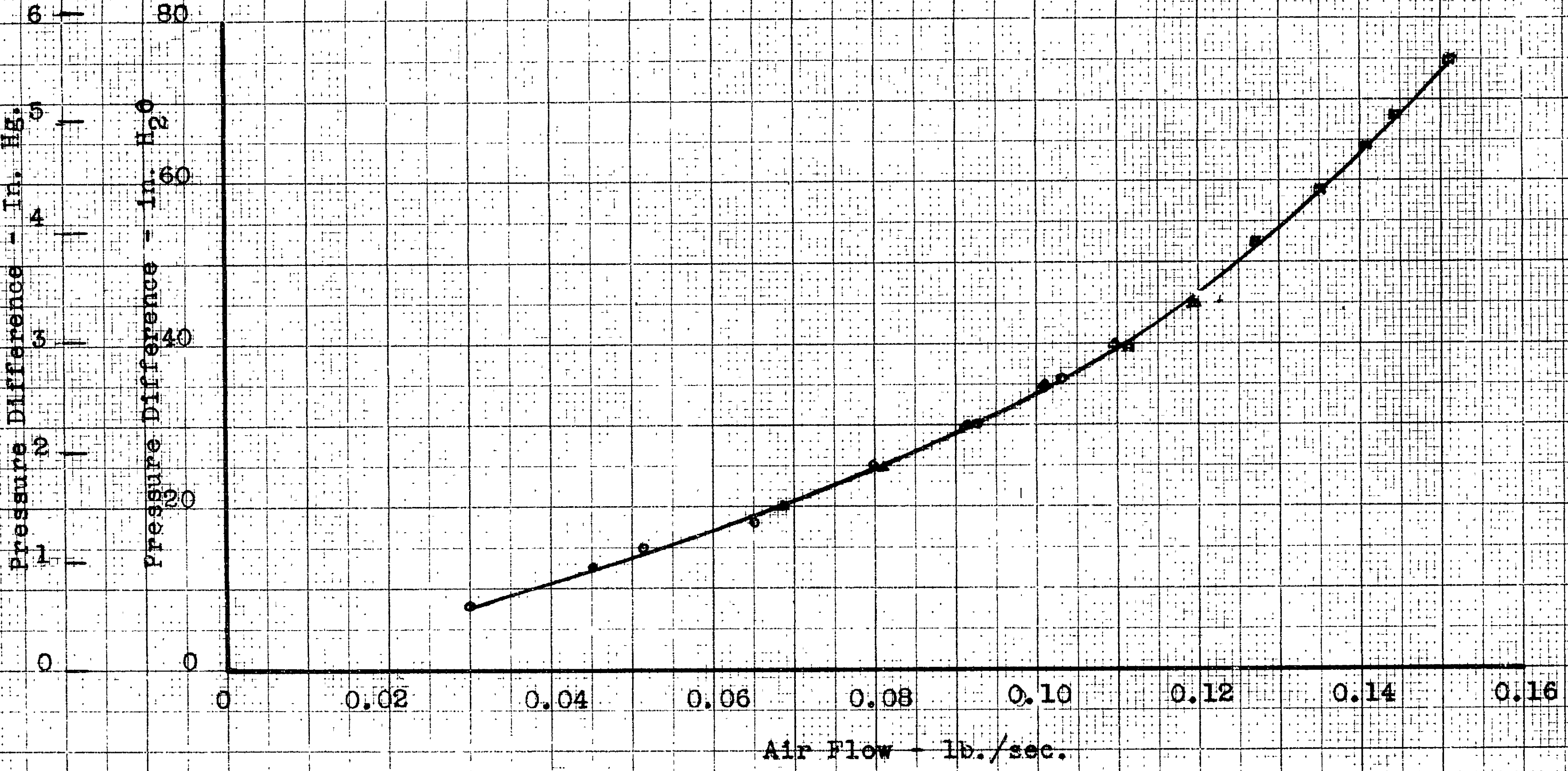

Figure 19

Pressure Difference across Reed Valves vs Air Flow

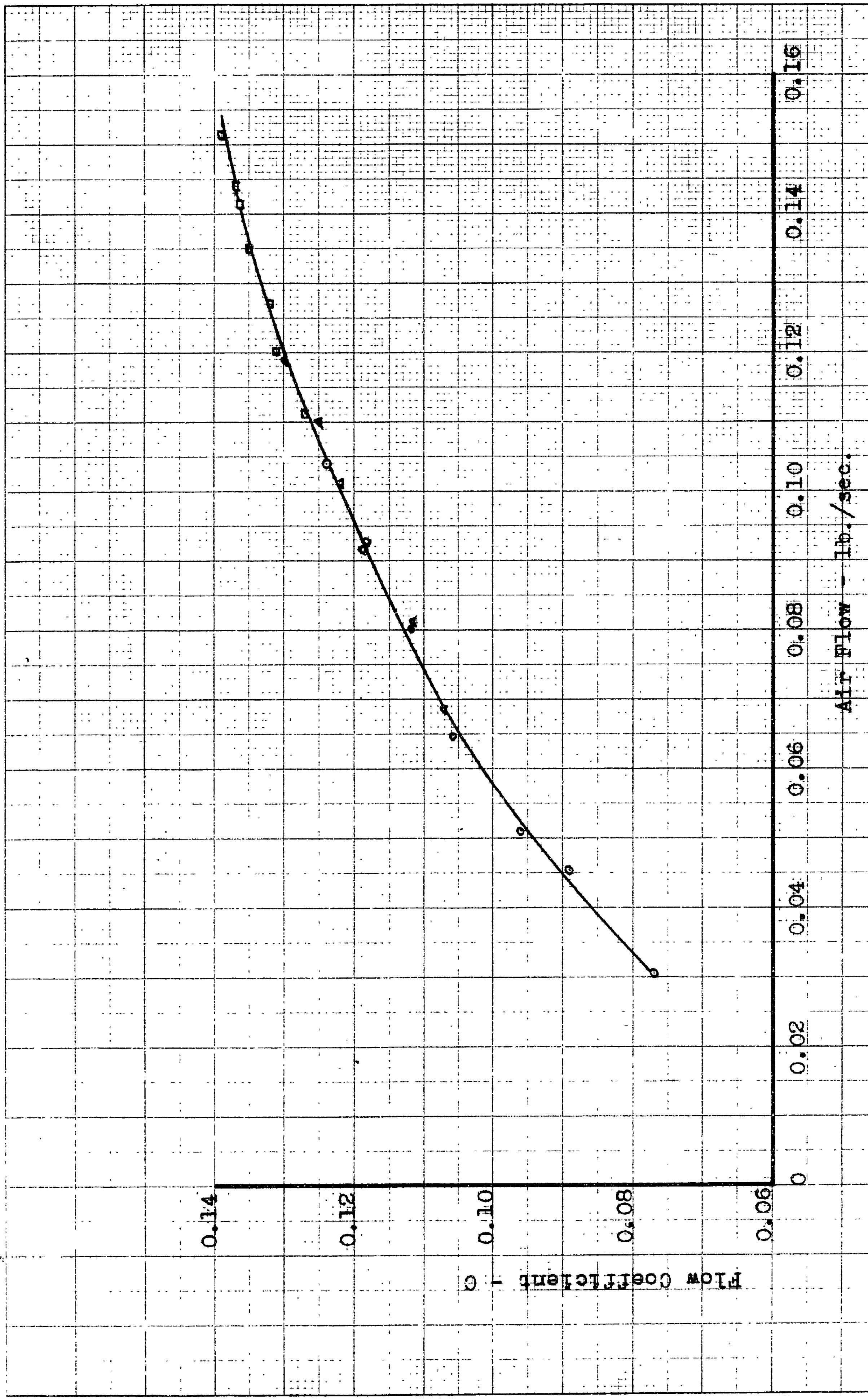

Figure 20

Steady Flow Coefficient vs Air Flow through Reed Valves

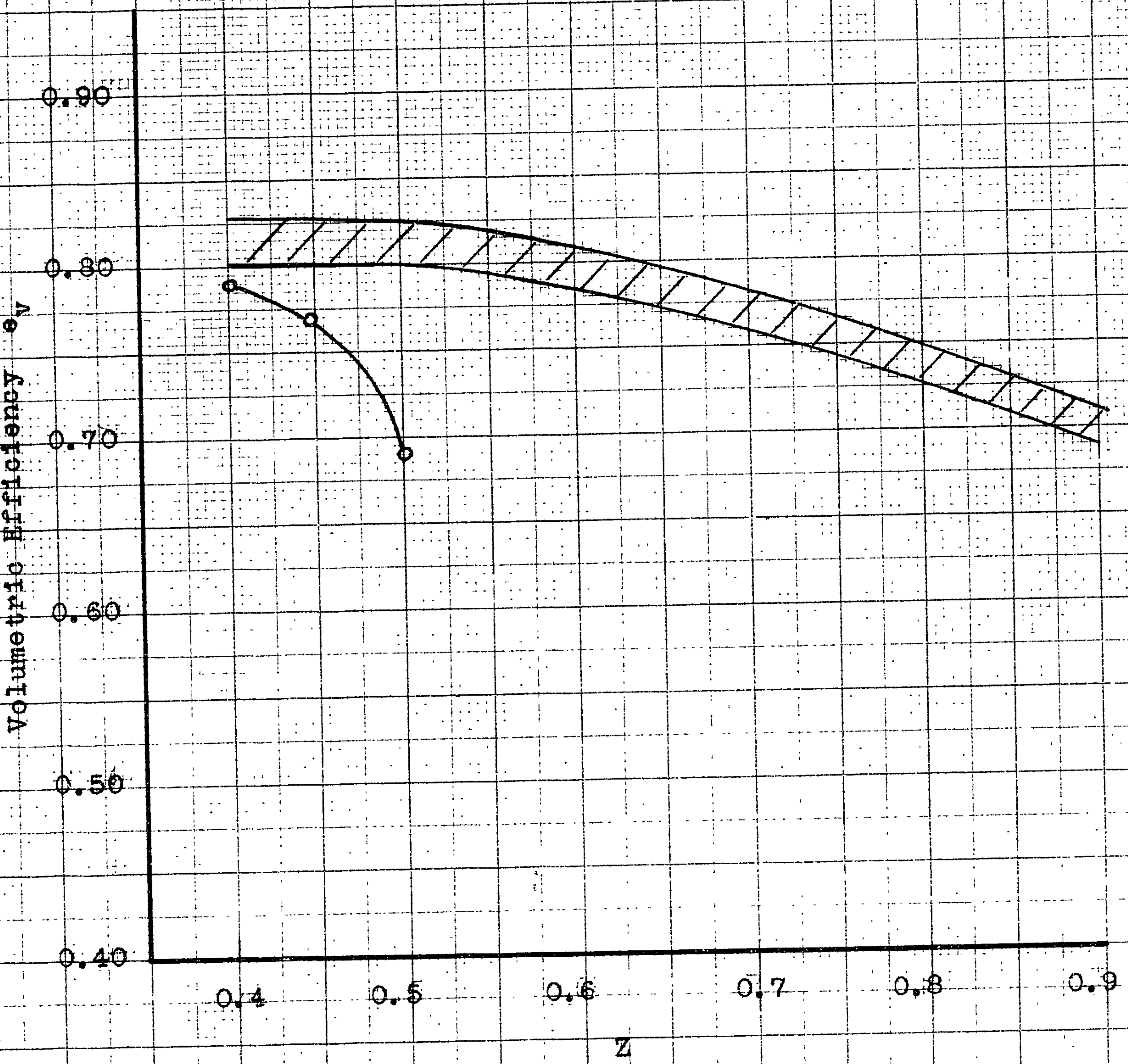

Figure 21

Volumetric Efficiency vs Z

Cross-hatched area denotes range of values for several four-stroke engines

Figure 22

STANDARD ATMOSPHERE TABLE

Z ft.	t °F	T °R	C ft/sec	$\frac{\rho}{\rho_o}$	$\sqrt{\frac{\rho}{\rho_o}}$	P in.Hg.	P lb/sq.in.	ρg lb/ft^3	$\mu \times 10^7$ $\frac{\text{lb. sec}}{\text{ft.}^2}$
0	59.0	518.4	1118	1.0000	1.0000	29.92	14.70	0.07651	3.66
1,000	55.4	514.8	1114	.9710	.9854	28.86	14.17	.07430	
2,000	51.8	511.3	1110	.9428	.9710	27.82	13.66	.07213	
3,000	48.3	507.7	1106	.9151	.9566	26.81	13.17	.07001	
4,000	44.7	504.1	1103	.8881	.9424	25.84	12.69	.06794	
5,000	41.2	500.6	1098	.8616	.9282	24.89	12.22	.06592	3.58
6,000	37.6	497.0	1094	.8358	.9142	23.98	11.77	.06395	
7,000	34.0	493.4	1091	.8106	.9003	23.09	11.34	.06202	
8,000	30.5	489.9	1087	.7859	.8865	22.22	10.90	.06013	
9,000	26.9	486.3	1082	.7619	.8729	21.38	10.50	.05829	
10,000	23.3	482.7	1078	.7384	.8593	20.58	10.10	.05649	3.50
11,000	19.8	479.1	1074	.7154	.8458	19.79	9.72	.05474	
12,000	16.2	475.6	1071	.6931	.8325	19.03	9.35	.05303	
13,000	12.6	472.0	1067	.6712	.8193	18.29	8.99	.05136	
14,000	9.1	468.5	1063	.6499	.8062	17.57	8.64	.04973	
15,000	5.5	464.9	1059	.6291	.7932	16.88	8.30	.04814	3.43
16,000	1.9	461.3	1055	.6088	.7803	16.21	7.97	.04658	
17,000	-1.6	457.8	1051	.5891	.7675	15.56	7.65	.04507	
18,000	-5.2	454.2	1047	.5698	.7549	14.94	7.34	.04359	
19,000	-8.8	450.6	1042	.5509	.7422	14.33	7.04	.04216	
20,000	-12.3	447.1	1038	.5327	.7299	13.75	6.76	.04075	3.34
21,000	-15.9	444.5	1034	.5148	.7175	13.18	6.48	.03938	
22,000	-19.5	439.9	1030	.4974	.7053	12.63	6.21	.03806	
23,000	-23.0	436.4	1026	.4805	.6932	12.10	5.94	.03676	
24,000	-26.6	432.8	1022	.4640	.6812	11.59	5.69	.03550	
25,000	-30.1	429.2	1017	.4480	.6693	11.10	5.46	.03427	3.24
26,000	-33.7	425.7	1013	.4323	.6575	10.62	5.22	.03308	
27,000	-37.3	422.1	1008	.4171	.6458	10.16	4.99	.03192	
28,000	-40.9	418.5	1004	.4023	.6343	9.72	4.77	.03078	
29,000	-44.4	415.0	999	.3879	.6228	9.29	4.56	.02968	
30,000	-48.0	411.4	995	.3740	.6116	8.88	4.36	.02861	3.14
31,000	-51.6	407.8	991	.3603	.6002	8.48	4.17	.02757	
32,000	-55.1	404.3	987	.3472	.5892	8.10	3.98	.02656	
33,000	-58.7	400.7	982	.3343	.5782	7.73	3.80	.02558	
34,000	-62.3	397.2	978	.3218	.5673	7.38	3.62	.02463	
35,000	-65.8	393.6	973	.3098	.5566	7.04	3.45	.02369	
36,000	-67.0	392.4	972	.2962	.5442	6.71	3.30	.02265	3.01
37,000	-67.0	392.4	972	.2824	.5314	6.39	3.14	.02160	
38,000	-67.0	392.4	972	.2692	.5188	6.10	2.99	.02059	
39,000	-67.0	392.4	972	.2566	.5066	5.81	2.85	.01963	
40,000	-67.0	392.4	972	.2447	.4950	5.54	2.72	.01872	3.01

Condensed from: Standard Atmosphere - Tables and Data. Technical Note No. 218, NACA, 1940. Diehl, Walter S.

APPENDIX A

Best Power Spark Advance

August 26, 1952

$p_e = p_i = 28.0$ in. Hg. abs. $t_i = 86°F$ $t_{plug} = 425°F$

$F_A = .078$

3500 rpm.

Ignition, degrees B.T.C.	Hydraulic Scale Reading - in.Hg.
27	21.00
32	21.20
37	21.30
40	21.10
42	21.10
37	21.45
32	21.35

4000 rpm.

Ignition, degrees B.T.C.	Hydraulic Scale Reading - in.Hg.
32	19.35
35	19.50
37	19.45
40	19.60
42	19.50
37	19.60
37	19.65

Plotted in Figure 9

Best Power Fuel-air Ratio

$p_e = p_i = 28.0$ in. Hg. abs. $t_i = 81°F$ $t_{plug} = 425°F$

Spark = 37 degrees B.T.C. 4000 rpm.

F_A	Hydraulic scale reading - in. Hg.
0.0694	19.40
.0707	19.70
.0722	19.65
.0740	19.75
.0756	20.10
.0776	20.20
.0792	20.15
.0822	20.10
.0878	19.95
.0939	19.90
.0997	19.60
.0782	20.15
.0729	20.10
.0697	19.70
.0663	18.80
.0777	20.00
.0664	16.50
.0629	15.10
.0579	11.00
.1174	19.20
.1174	18.80

Best power F_A from above data = 0.078

Change in Observed Best Power Fuel Air Ratio

with Inlet Pressure

October 6, 1952

$p_e = p_i = 20.0$ in. Hg. abs. $t_i = 82°F$ $t_{plug} = 425°F$

Spark = 37° B.T.C. 3500 rpm.

F_A	Hydraulic scale reading, in. Hg.
0.0735	14.4
.0805	15.2
.0883	15.5
.0955	15.5
.1020	15.3

Best power F_A from above data = 0.092

Summary of Performance with Old-type Reed Valves

September 23 to October 1, 1952

(Average of four sets of runs under same conditions)

$p_e = p_i$ = 27.3 in. Hg. absolute

Spark = 37° b.t.c. t_i = 80°F t_{plug} = 425°F

F_A = 0.078 p_o = 30.0 in. Hg. abs. t_o = 78°F

rpm	3400	4000	4400
Rotameter, cm	7.90	8.00	8.50
Dynamometer, firing, in. Hg.	22.20	19.80	18.80
Dynamometer, motoring, in. Hg.	4.17	4.45	4.85
Δh, in. H_2O	28.4	29.6	35.8
p_{duct}, in. H_2O	8.2	8.9	11.4
$\dot{M}_a$, lbs/sec.	0.0450	0.0460	0.0506
$\dot{M}_f$, lbs/sec.	0.00351	0.00359	0.00395
bmep	66.4	59.2	56.2
fmep	12.5	13.3	14.5
imep	78.9	72.5	70.7
bhp	15.10	15.85	16.56
fhp	2.83	3.56	4.26
ihp	17.9	19.4	20.8
R_s	0.69	0.60	0.60
e_{ve}	0.77	0.67	0.67
bsfc	0.84	0.82	0.86

Note: These runs were made at 3400, 4000 and 4400 rpm due to an error in speed determination with stroboscope.

Observed Best Power Fuel Air Ratio at Several Inlet Pressures

November 17 - 18, 1952

Spark = 37° B.T.C. 3500 rpm.

$p_e = p_i = 27.3$ in. Hg. abs., $t_i = 76°F$, $t_{plug} = 400°F$

F_A	Hydraulic Scale reading, in. Hg.
0.0676	21.60
.0689	22.20
.0706	22.60
.0736	22.90
.0765	23.00
.0792	23.00
.0823	22.95
.0848	22.85
.0875	22.80
.0905	22.70
.0954	22.60

$p_e = p_i = 20.0$ in. Hg. abs. $t_i = 76°F$, $t_{plug} = 400°F$

0.0715	15.50
.0735	15.70
.0755	15.95
.0798	16.20
.0839	16.20
.0881	16.15
.0922	16.00
.100	15.90

$p_e = p_i = 15.0$ in. Hg. abs. $t_i = 74°F$, $t_{plug} = 350°F$

F_A	Hydraulic scale, in. Hg.
0.0663	8.90
.0684	9.40
.0706	9.90
.0730	10.20
.0750	10.60
.0801	10.95
.0848	10.95
.0887	10.90
.0941	10.90
.100	10.70
.109	10.55

$p_e = p_i = 11.5$ in. Hg. abs. $t_i = 74°F$, $t_{plug} = 300°F$

0.0716	6.60
.0744	6.90
.0770	7.10
.0801	7.20
.0834	7.25
.0890	7.30
.0950	7.25
.101	7.15
.107	7.00
.117	6.85

Plotted in Figure 10

$p_e = p_i = 11.5$ in. Hg. absolute

November 18, 1952

Spark = 37° b.t.c. $t_i = 76°F$ $t_{plug} = 300°F$

observed $F_A = 0.086$ $p_o = 30.0$ in. Hg. abs. $t_o = 74°F$

rpm	3400	4000	4400
Rotameter, cm.	4.90	5.30	5.00
Dynamometer, firing, in. Hg.	6.55	5.80	4.10
Dynamometer, motoring, in. Hg.	3.45	4.50	4.75
Δh, in. H_2O	4.6	5.8	5.1
p_{duct}, in. H_2O	6.1	8.4	8.0
$\dot{m}_a$, lbs/sec.	0.0182	0.0204	0.0190
$\dot{m}_f$, lbs/sec.	0.001575	0.00176	0.00163
bmep	19.8	17.3	12.3
fmep	10.3	13.5	14.2
imep	30.1	30.8	26.5
bhp	4.45	4.64	3.61
fhp	2.34	3.60	4.18
ihp	6.8	8.2	7.8
R_s (observed)	0.661	0.630	0.534
R_s (corrected for leakage)	0.72	0.69	0.58
e_s	0.37	0.38	0.33
e_{vc}	0.80	0.78	0.64

<u>Correction for altitude temperature</u>

24,000 ft. $t = -27°F$ $\rho = 0.0354$ lbs/cu.ft.

ihp	7.6	9.1	8.7
bhp	5.3	5.5	4.5
bmep	23.3	20.6	15.3
$\dot{m}_f$, lbs/sec.	0.001752	0.00196	0.001812
bsfc	1.19	1.27	1.45
$\eta_{mech.}$	0.70	0.60	0.52

Note: These runs were made at 3400, 4000 and 4400 rpm due to an error in speed determination with stroboscope.

$p_e = p_i = 15.0$ in. Hg. absolute

November 19, 1952

Spark = 37° b.t.c. t_i = 76°F t_{plug} = 350°F

observed F_A = 0.0835 p_o = 30.0 in. Hg. abs. t_o = 74°F

rpm	3500	4000	4500
Rotameter, cm.	5.85	6.20	5.80
Dynamometer, firing, in. Hg.	9.70	8.80	6.30
Dynamometer, motoring, in. Hg.	3.80	4.50	4.70
Δh, in. H_2O	8.5	10.6	8.6
p_{duct}, in. H_2O	5.0	6.8	6.8
$\dot{M}_a$, lbs/sec.	0.0247	0.0276	0.0248
$\dot{M}_f$, lbs/sec.	0.00206	0.00231	0.00208
bmep	29.0	26.3	18.8
fmep	11.4	13.5	14.1
imep	40.4	39.8	32.9
bhp	6.80	7.05	5.67
fhp	2.66	3.60	4.23
ihp	9.5	10.7	9.9
R_s (observed)	0.668	0.654	0.522
R_s (corrected for leakage)	0.71	0.69	0.55
e_s	0.38	0.38	0.31
e_{vc}	0.79	0.77	0.61

<u>Correction for altitude temperature</u>

18,000 ft, $t = -5$°F $\rho = 0.0438$ lbs/cu.ft.

ihp	10.3	11.6	10.7
bhp	7.6	8.0	6.5
bmep	32.4	29.9	21.6
$\dot{M}_f$, lbs/sec.	0.002235	0.00250	0.00226
bsfc	1.06	1.13	1.25
$\eta_{mech.}$	0.74	0.69	0.60

$p_e = p_i$ = 20.0 in. Hg. absolute

November 20, 1952

Spark = 37° b.t.c. t_i = 76°F t_{plug} = 400°F

observed F_A = 0.0835 p_o = 30.0 in. Hg. abs. t_o = 74°F

rpm	3500	4000	4500
Rotameter, cm.	6.85	7.30	7.10
Dynamometer, firing, in. Hg.	14.60	13.70	10.80
Dynamometer, motoring, in. Hg.	3.90	4.80	4.90
Δh, in. H_2O	15.7	19.6	17.8
p_{duct}, in. H_2O	5.5	6.8	8.0
$\dot{M}_a$, lbs/sec.	0.0336	0.0376	0.0358
$\dot{M}_f$, lbs/sec.	0.00280	0.00314	0.00299
bmep	43.6	41.0	32.3
fmep	11.2	14.4	14.7
imep	54.8	55.4	47.0
bhp	10.22	10.97	9.73
fhp	2.75	3.84	4.41
ihp	13.0	14.8	14.1
R_s (observed)	0.683	0.668	0.565
R_s (corrected for leakage)	0.72	0.70	0.60
e_s	0.39	0.39	0.33
e_{vc}	0.80	0.78	0.67

<u>Correction for altitude temperature</u>

10,750 ft. t = 20°F ρ = 0.0554 lbs/cu.ft.

ihp	13.7	15.6	14.9
bhp	11.0	11.8	10.5
bmep	47.0	44.0	34.9
$\dot{M}_f$, lbs/sec.	0.002955	0.003315	0.003155
bsfc	0.97	1.01	1.05
η mech.	0.80	0.76	0.70

$p_e = p_i = 27.2$ in. Hg. absolute

November 20, 1952

Spark = 37° b.t.c. $t_i = 76°F$ $t_{plug} = 400°F$

$F_A = 0.079$ $p_o = 30.0$ in. Hg. abs. $t_o = 74°F$

rpm	3500	4000	4500
Rotameter, cm.	8.20	8.85	9.00
Dynamometer, firing, in. Hg.	21.10	20.40	18.40
Dynamometer, motoring, in. Hg.	4.40	5.40	5.60
Δh, in. H_2O	31.2	38.5	39.7
p_{duct}, in. H_2O	12.0	13.5*	13.5*
$\dot{M}_a$, lbs/sec.	0.0474	0.0527	0.0535
$\dot{M}_f$, lbs/sec.	0.00374	0.00416	0.00423
bmep	63.1	61.0	55.0
fmep	13.2	16.2	16.8
imep	76.3	77.2	71.8
bhp	14.80	16.32	16.57
fhp	3.08	4.32	5.04
ihp	17.9	20.6	21.6
R_s (observed) = R_s (corrected for leakage)	0.71	0.69	0.62
e_s	0.40	0.40	0.37
e_{vc}	0.78	0.77	0.69

* $t_{plug} = 425°F$

<u>Correction for altitude temperature</u>

3500 ft. $t = 50°F$ $\rho = 0.0709$ lbs/cu.ft.

ihp	18.3	21.1	22.1
bhp	15.2	16.8	17.1
bmep	65.0	62.7	56.8
$\dot{M}_f$, lbs/sec.	0.00383	0.00426	0.00433
bsfc	0.91	0.91	0.91
η_{mech}	0.83	0.80	0.81

p_e = 20.0 in. Hg. abs., p_i = 22.0 in. Hg. abs.

November 24, 1952

Spark = 37° b.t.c. t_i = 76°F t_{plug} = 400°F

observed F_A = 0.0835 p_o = 30.0 t_o = 76°F

rpm	3500	4000	4500
Rotameter, cm.	8.20	8.60	8.70
Dynamometer, firing, in. Hg.	17.10	16.20	14.50
Dynamometer, motoring, in. Hg.	4.00	4.50	5.20
Δh, in. H_2O	27.8	32.1	33.4
p_{duct}, in. H_2O	8.0	8.5	11.0
$\dot{M}_a$, lbs/sec.	0.0447	0.0480	0.0489
$\dot{M}_f$, lbs/sec.	0.00374	0.0040	0.00408
bemp	51.1	48.5	43.4
fmep	12.0	13.5	15.6
imep	63.1	62.0	59.0
bhp	12.0	13.0	13.05
fhp	2.8	3.6	4.7
ihp	14.8	16.6	17.8
R_s (observed)	0.908	0.854	0.772
R_s (corrected for leakage)	0.96	0.90	0.82
e_s	0.45	0.44	0.42
e_{vc}	0.91	0.86	0.78

<u>Correction for altitude temperature</u>

10,750 ft. t = 20°F ρ = 0.0554 lbs/cu.ft.

ihp	15.6	17.5	18.8
bhp	12.8	13.9	14.1
bmep	54.7	51.9	46.7
$\dot{M}_f$, lbs/sec.	0.00395	0.00422	0.00430
bsfc	1.11	1.09	1.10
η mech.	0.82	0.79	0.75

Flow Test of Reed Valves

December 4, 1952

Orifice Diameter 0.725 in. $t_i = t_o = 72°F$

Δp_{reed}	p_i	p_e	p_o	Δh	$\dot{M}_a$	p_e/p_i	ϕ_2	ρ_i	C
in.H_2O	in.Hg.abs.	in.Hg.abs.	in.H_2O	in.H_2O	lbs/sec.			lbs/cu.ft.	
8.10	29.00	28.40	29.90	13.00	0.0306	0.980	0.158	0.0725	0.077
12.85	27.86	26.90	29.90	28.45	0.0454	0.966	0.210	0.0696	0.089
14.96	27.28	26.18	29.80	36.20	0.0511	0.959	0.225	0.0681	0.096
Orifice Diameter = 1.447 in.									
18.60	29.20	27.90	29.70	2.67	0.0649	0.955	0.240	0.0730	0.106
24.75	28.80	26.96	29.60	4.10	0.0803	0.936	0.287	0.0720	0.112
30.40	28.40	26.16	29.50	5.46	0.0925	0.921	0.317	0.0710	0.118
36.25	28.00	25.30	29.35	6.90	0.1038	0.904	0.345	0.0700	0.124
December 6, 1952									
20.14	28.81	27.30	29.45	3.00	0.0685	0.948	0.255	0.0720	0.107
25.25	28.47	26.58	29.30	4.20	0.0810	0.934	0.290	0.0711	0.113
30.05	28.12	25.89	29.20	5.38	0.0915	0.922	0.315	0.0703	0.119
34.95	27.78	25.17	29.10	6.59	0.1010	0.906	0.343	0.0694	0.122
39.75	27.42	24.45	29.00	7.81	0.1098	0.891	0.367	0.0685	0.125
45.60	27.01	23.60	28.85	9.28	0.1193	0.874	0.390	0.0675	0.130
December 11, 1952									
39.7	27.50	24.55	29.05	7.85	0.1110	0.893	0.365	0.0687	0.127
46.55	27.05	23.69	28.90	9.41	0.1202	0.874	0.390	0.0675	0.131
54.2	26.70	22.82	28.80	10.62	0.1273	0.856	0.415	0.0667	0.132
58.9	23.30	21.94	28.65	12.01	0.1353	0.835	0.438	0.0657	0.135
64.4	26.00	21.23	28.60	13.05	0.1410	0.817	0.457	0.0650	0.136
68.2	25.80	20.75	28.50	13.74	0.1442	0.805	0.468	0.0645	0.137
75.4	25.41	19.83	28.40	15.07	0.1510	0.780	0.490	0.0635	0.139

APPENDIX B

Method of correction for temperature

$$e_v = \frac{\dot{M}_a}{\rho_i V_d N}$$ (for a four-stroke engine or for the crankcase of the two-stroke).

where $\dot{M}_a$ and ρ_i are based on conditions at the inlet to the crankcase, p_i and T_i. When T_i changes, $\rho_i \sim \frac{1}{T_i}$

But it has been determined experimentally that, for a four-stroke engine

$$\dot{M}_a \sim \frac{1}{\sqrt{T_i}}$$

because of heat transfer effects. For example, suppose T_i is cut in half. Due to the greater temperature differential between the air and the hot engine parts it comes in contact with, the rate of heat transfer to the air is increased and while theoretically $\dot{M}_a$ would be doubled, the actual increase is only 1.4, hence,

$$e_v \sim \frac{\frac{1}{\sqrt{T_i}}}{\frac{1}{T_i}} \sim \sqrt{T_i}$$

Since the inlet process of the crankcase scavenged engine is similar to that of the four-stroke in the respect of opportunity for heat transfer to the fresh mixture, it is believed that the above relation is a good approximation.

$$R_s = \frac{\dot{M}_{a\,\text{ports}}}{\rho_s V_d \frac{r}{r-1} N}$$

Theoretically, ρ_s is at the temperature of the mixture entering the cylinder inlet port, T_p, and the pressure at the exhaust port. Since T_p was not known, T_i has been used for all R_s calculations. However, by the same reasoning regarding heat transfer effects, it appears that $T_p \sim \sqrt{T_i}$. A change in T_i would not be expected to result in the same magnitude of change in T_p, since the mixture must undergo compression in the crankcase before it reaches the port. Therefore, if T_p is assumed to be proportional to $\sqrt{T_i}$, $\rho_s \sim \frac{1}{\sqrt{T_i}}$

$\dot{M}_a$ ports $\equiv \dot{M}_a$ crankcase

Hence $\dot{M}_a$ ports $\sim \frac{1}{\sqrt{T_i}}$

Therefore :

$$R_s \sim \frac{\frac{1}{\sqrt{T_i}}}{\frac{1}{\sqrt{T_i}}} = \text{const. with respect to } T_i$$

The general equation for power output of a two-stroke engine is:

$$IHP = N \frac{V_d}{1728} \frac{r}{r-1} \rho_s \, e_s \, F_A E_c \, \eta_i \, \frac{778}{33{,}000}$$

If R_s is constant with temperature e_s is constant with temperature and the only variable is ρ_s, which is proportional to $\frac{1}{\sqrt{T_i}}$

$$\text{Therefore: } IHP_{alt.} = IHP_{test} \sqrt{\frac{T_i}{T_{alt.}}}$$

APPENDIX C

Sample Calculation

This set of calculations has been carried out for the condition of $p_e = p_i$ = 20 in.Hg.abs. and 4000 rpm. It is typical of those carried out for all other points.

(a) $\dot{M}_a = 0.1145\ D_o^2\ KY \sqrt{\frac{p_o}{T_o} \Delta h}$

where K is the flow coefficient, a function of Reynolds number, and Y is a correction for expansion. (See Sloan Laboratory Air Flow Notes)

$$\dot{M}_a = 0.1145\ (0.725)^2(0.608)(0.982) \sqrt{\frac{30}{534}\ (19.6)}$$

$$\dot{M}_a = 0.0376 \text{ lb. per sec.}$$

(b) $\dot{M}_f = F_A\ (\dot{M}_a)$

$$= 0.0835\ (0.0376) = 0.00314 \text{ lb.per sec.}$$

(c) $\text{bmep} = \dfrac{396{,}000\ h_f}{K\ V_d}$

where h_f is the hydraulic scale reading in inches of mercury and K is the overall dynamometer constant. (See Sloan Laboratory Dynamometer Notes)

$$= \frac{396{,}000\ (13.70)}{5000\ (26.5)} = 41.0 \text{ psi}$$

(d) $\text{fmep} = \dfrac{396{,}000\ h_m}{K\ V_d}$

$$= \frac{396{,}000\ (4.80)}{5000\ (26.5)} = 14.4 \text{ psi}$$

(e) imep = bmep + fmep

$$= 41.0 + 14.4 = 55.4 \text{ psi}$$

(f) $bhp = \dfrac{Nh_f}{K}$

$$= \frac{4000\ (13.70)}{5000} = 10.97$$

(g) $fhp = \dfrac{Nh_m}{K}$

$$= \frac{4000\ (4.80)}{5000} = 3.84$$

(h) ihp = bhp + fhp

$$= 10.97 + 3.84 = 14.8$$

(i) $R_s\ (\text{observed}) = \dfrac{\dot{M}_a}{\rho_s \left(\frac{N}{60}\right)\left(\frac{V_d}{1728}\right)\left(\frac{r}{r-1}\right)}$

where $\rho_s = \dfrac{p_e\ m}{R\ T_i}$

$$= \frac{20\ (70.8)\ (29)}{1545\ (536)} = 0.0495 \text{ lb/ft}^3$$

$$R_s = \frac{0.0376}{0.0495 \left(\frac{4000}{60}\right)\left(\frac{26.5}{1728}\right)\left(\frac{10}{9}\right)}$$

$$= 0.668$$

(j) $R_s\ (\text{corrected for leakage}) = \dfrac{\dot{M}_a \left[\frac{F_{A\ (observed)}}{0.079}\right]}{\rho_s \left(\frac{N}{60}\right)\left(\frac{V_d}{1728}\right)\left(\frac{r}{r-1}\right)}$

$$= \left[\frac{F_{A\ (observed)}}{0.079}\right] R_{s\ observed}$$

$$= \frac{0.0835}{0.079}\ (0.668) = 0.70$$

(k) Calculation of e_s is illustrated in Appendix D

(l) $$e_{vc} = \frac{\dot{M}_a}{\rho_i \left(\frac{N}{60}\right)\left(\frac{V_d}{1728}\right)}$$

where $p_e = p_i$:

$$e_{vc} = \left(\frac{r}{r-1}\right) R_s$$

$$= \left(\frac{10}{9}\right)(0.70) = 0.78$$

(m) $$\text{Altitude ihp} = \text{ihp} \sqrt{\frac{T_i}{T_{alt.}}}$$

$$= 14.8 \sqrt{\frac{536}{480}} = 15.6$$

(n) Altitude bhp = ihp - fhp

$$= 15.6 - 3.84 = 11.8$$

(o) $$\text{Altitude bmep} = \frac{\text{bhp}_c\ (12)(33{,}000)}{N\ V_d}$$

$$= \frac{11.8\ (12)(33{,}000)}{4000\ (26.5)} = 44.0 \text{ psi}$$

(p) $$\text{Altitude } \dot{M}_f = \dot{M}_f \sqrt{\frac{T_i}{T_{alt.}}}$$

$$= 0.00314 \sqrt{\frac{536}{480}} = 0.003315 \text{ lb/sec.}$$

(q) $$\text{Altitude bsfc} = \frac{\text{alt.} \dot{M}_f\ (3600)}{\text{alt. bhp}}$$

$$= \frac{0.003315\ (3600)}{11.8} = 1.01 \text{ lb/bhp-hr.}$$

(r) $$\text{Mechanical efficiency, } \eta_{mech.} = \frac{\text{bhp}}{\text{ihp}}$$

$$= \frac{11.8}{15.6} = 0.76$$

APPENDIX D

Estimation of scavenging efficiency

The indicated efficiency of any engine is primarily a function of compression ratio, fuel-air ratio and spark advance. It is not a function of speed or inlet pressure. Hence, it may be assumed that since best power fuel-air ratio and spark advance was used for all test points, the indicated efficiency was constant for all points. It should be noted that this indicated efficiency is based upon the fuel-air mixture actually used in combustion and not upon the measured fuel and air consumption of the engine. The general equation for the indicated power output of a two-stroke engine is

$$IHP = \left[N \frac{V_d}{1728} \frac{r}{r-1} \rho_s e_s \right] F_A E_c \eta_i \frac{778}{33,000}$$

where the quantity in the brackets is $\dot{M}_a'$, the mass of air retained, and F_A is the true fuel-air ratio.

The value of η_i was determined by means of a fuel-air cycle calculation using the Hottel charts for an engine operating at the same conditions as the two-stroke. The method is discussed in Taylor and Taylor and only the calculation is included here.

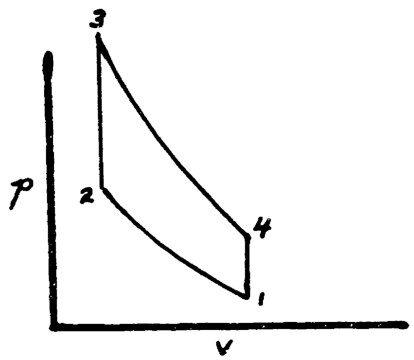

$p_e = p_i = 27.2$ in.Hg.abs. $= 13.4$ psia

$T_i = 536$ °R

$F_A = 0.079$

$T_{residual\ gas} = 2250$°R (assumed)

f (weight ratio of residual gas to total charge) = 4% (assumed)

$H_{s_1} = 40\ (1-f) + 590\ f$

$= 40\ (.96) + 590\ (.04)$

$= 62$ Btu.

$T_1 = 605$°R $V_1 = 18.0\ ft^3$ $E_{s_1} = 20$ Btu

$V_2 = 18/10 = 1.8$ $p_2 = 270_{psia}$ $T_2 = 1260$°R $E_{s_2} = 163$ Btu

$E_c = 1507\ (1-f) + 300\ (f)$

$= 1507\ (.96) + 300\ (.04)$

$= 1459$ Btu

$E_3 = 1459 + 163 = 1622$ Btu

$V_3 = 1.8\ ft^3$ $p_3 = 1200$ psia $T_3 = 5100$°R

$V_4 = 18\ ft^3$ $p_4 = 69$ psia $T_4 = 2980$°R $E_4 = 913$ Btu

$$\text{work} = (E_3 - E_4) - (E_2 - E_1)$$

$$= (1622 - 913) - (163 - 20)$$

$$= 566 \text{ Btu}$$

$$\eta_o = \frac{566}{.96(1507)} = .392$$

The ratio of the indicated efficiency actually attained to the fuel-air cycle efficiency varies from .80 to .90 with different engines. The value of .80 was chosen as a realistic assumption. Hence,

$$\eta_i = .80\,\eta_o$$

$$= .80\,(.392)$$

$$= .314$$

This value of η_i represents the efficiency with which the fuel-air mixture which is trapped in the cylinder is converted into work.

To evaluate the scavenging efficiency, the general equation for indicated power output is solved for e_s at each test point, using the value of ihp determined from the test data. For example, at the condition of $p_e = p_i = 20$ in.Hg.abs. and 4000 rpm:

$$\text{IHP} = 14.8, \quad \rho_s = \frac{p_e\,m}{R\,T_i} = \frac{20(70.8)(29)}{1545\,(536)} = 0.0495 \text{ lb/ft}^3$$

True $F_A = 0.079$ $\quad E_c = 19{,}200$ Btu/lb.

$$e_s = \frac{\text{IHP}\,(1728)\,(33000)}{N\,V_d\,\frac{r}{r-1}\,\rho_s\,F_A E_c\,\eta_i\,778}$$

$$= \frac{14.8\,(1728)\,(33{,}000)}{4000\,(26.5)\,(\frac{10}{9})\,(0.079)\,(19{,}200)\,(0.314)\,(778)}$$

$$= .39$$

APPENDIX E

Calculation of Steady Flow Coefficient and Gulp Factor

The general equation for flow through an orifice is

$$\dot{M}_a = A\ C\ c_{si} \rho_i\ \phi_2$$

where ϕ_2 is $\left\{ \frac{2}{k-1} \left[\left(\frac{p_2}{p_1}\right)^{\frac{2}{k}} - \left(\frac{p_2}{p_1}\right)^{\frac{k+1}{k}} \right] \right\}^{1/2}$

and is used when p_2/p_1 is greater than 0.528 (greater than critical) The value of ϕ_2 is plotted against P_2/p_1 in figure 18. In the flow tests of the reed valves, $p_i = p_1$ and $p_e = p_2$. The velocity of sound in the inlet air is found from the expression

$$c_{si} = \sqrt{\frac{g\ R\ T\ k}{m}}$$

$$= \sqrt{\frac{32.2\ (1545)\ (532)\ (1.4)}{29}}$$

$$= 1135 \text{ ft.per sec.}$$

The flow equation is solved for C using the measured value of $\dot{M}_a$ determined in the test. For example, the last test point, $\Delta p_{reed} = 75.4$ inches of H_2O, is calculated as follows:

as before,

$$\dot{M}_a = 0.1145\ D_o^2\ K\ Y \sqrt{\frac{P_o}{T_o} \Delta h}$$

$$= 0.1145\ (1.447)^2\ (.705)\ (.995) \sqrt{\frac{28.4}{532}\ (15.07)}$$

$$= 0.1510 \text{ lb. per sec.}$$

$$p_e/p_i = \frac{p_2}{p_1} = \frac{19.83}{25.41} = 0.780$$

from figure 18, $\phi_2 = 0.490$

The area used is the total area of the reed valve ports and the inlet density is 0.0635 lb/ft^3

$$C = \frac{\dot{M}_a}{A_v\, c_{si} \rho_i\, \phi_2}$$

$$= \frac{0.1510}{\left(\frac{4.42}{144}\right)(1135)\ (0.0635)\ (0.490)}$$

$$= 0.139$$

Values of C computed in this manner are plotted vs $\dot{M}_a$ in Figure 20.

For a four-stroke engine,

$$\text{Gulp factor, } Z = \frac{\frac{s}{60}}{c_{si}}\ \frac{A_p}{A_v}\ \frac{1}{C_{av}}$$

where C_{av} is the average flow coefficient of the valve. If it is assumed that the duration reed is open is 150° of crank angle, the average flow during the inlet cycle is the observed flow, $\dot{M}_a$, divided by 150/360. For example, Z at the condition of $p_e = p_i =$ 27.2 in.Hg.abs. and 4000 rpm is determined as follows:

$$\dot{M}_a = 0.0527 \text{ lb.per sec.}$$

$$\text{average flow} = 0.0527 \left(\frac{360}{150}\right) = 0.125 \text{ lb.per sec.}$$

$$\text{from figure 20, C at this flow} = 0.131 = C_{av}$$

$$Z = \frac{\left(\frac{1832}{60}\right)}{1135}\ \frac{9.62}{4.42}\ \frac{1}{0.131}$$

$$= 0.446$$

Note that the steady flow coefficient must be determined at a value of p_i near the test condition of inlet pressure for which Z is to be evaluated. Hence, figure 20 gives only values of C_{av} applicable to runs at $p_e = p_i = 27.2$ in.Hg.abs. Steady flow tests with p_i throttled to a lower value would be required to determine C_{av} and z for conditions of lower inlet pressure.

APPENDIX F

Inertia Forces on Connecting Rod

Weight of piston, pin and rod		5.38 lbs.
crank radius	r	1.375 inches
connecting rod length,	ℓ	5.5 inches

$$F_{max.} = \frac{W}{g} a = \frac{W}{g} \left[r\omega^2 \left(1 + \frac{r}{\ell}\right) \right]$$

$$\text{at } 4500 \text{ rpm, } \omega = 2\pi\left(\frac{4500}{60}\right) = 472$$

$$F_{max.} = \frac{5.38}{32.2} \left[\frac{1.375}{12} (472)^2 \left(1 + \frac{1.375}{5.5}\right) \right]$$

$$= 5320 \text{ lbs.}$$

The piston area is 9.62 in^2. Since the maximum gas pressure at sea level probably does not exceed 500 psi,

max. gas force = 500(9.62) = 4800 lb.

Hence, it appears that the inertia force is always greater than the gas force at this (maximum) speed and the rod would be subjected to a stress reversal each cycle.

APPENDIX G

Discussion of Air Leakage into Crankcase

When the pressure in the inlet tank (and the crankcase) was reduced to below atmospheric, it was noted that the observed fuel-air ratio for best power changed. The tabulated data in Appendix A shows this effect; at near sea level inlet pressure the best power ratio was 0.078 while at an inlet pressure of 20 in.Hg.abs. the ratio appeared to be 0.092. Since the actual fuel-air ratio for best power is known to be essentially independent of inlet pressure, it was obvious that a quantity of air was being inducted into the engine which was not being measured. The primary source of leakage appeared to be the seals at the ends of the crankshaft. These were not designed to operate under appreciable pressure differences; in operation the engine inducts its air at the pressure of its surroundings and the pressure fluctuations in the crankcase are so rapid as to make leakage at the seals negligible. However, in simulating altitude conditions in the laboratory, the inlet and exhaust pressures are below atmospheric while the engine is surrounded by air at sea level pressure. Hence, there is a constant pressure difference between the inside and outside of the engine crankcase in addition to the fluctuating pressure caused by the crankcase compression. Figure 1, showing the porting arrangement, illustrates how this can occur.

It is likely that the performance of the engine is affected differently by air obtained from leakage rather than from the actual inlet system. It was, therefore, desired to reduce the leakage to a minimum rather than to correct for it. The method used to accomplish this was discussed in Section III, Apparatus, and the degree to which it was successful is shown in figure 10. This indicates that a small amount of leakage was still present and figure 10 was used to form a correction factor for it. The amount of leakage was taken as being proportional to the change in the observed best power fuel-air ratio, assuming the observed ratio at an inlet pressure of 27.2 in.Hg.abs. to be the true best power ratio. Since the top of a fuel-air ratio curve is too flat to define an exact value, the comparison was made at the point of 98% maximum load on each curve. The fuel-air ratios so determined were then multiplied by 1.1 to obtain the best power value for each inlet pressure condition. These values were noted in Section IV, Test Procedure, and are referred to as the observed fuel-air ratio for best power. It should be noted that the actual fuel-air ratio in the engine is now assumed constant for all inlet pressures at 0.079.

REFERENCES

1. Taylor, C. F. and Taylor, E. S., The Internal Combustion Engine. International Textbook Company, 1948 p. 270.

2. Taylor and Taylor, op.cit. p. 251

3. Rogowski, A. R. and Bouchard, C. L., "Scavenging a Piston-ported Two-Stroke Cylinder" NACA Technical Note No. 674, 1938.

4. Livengood, J. C. and Stanitz, J. D., "The Effect of Inlet Valve Design, Size, and Lift on the Air Capacity and Output of a Four-Stroke Engine". NACA Technical Note No. 915, 1943.

BIBLIOGRAPHY

Taylor, C. F. and Taylor, E. S. The Internal Combustion Engine, International Textbook Company, 1948.

Rogowski, A. R. and Bouchard, C. L. "Scavenging a Piston-Ported Two-Stroke Cylinder". NACA Technical Note No. 674, 1938.

Rogowski, A. R., "Possibilities of the Two-Stroke Cycle for Small Aircraft" Journal of the Aeronautical Sciences, April, 1941.

Toong, T. Y. and Tsai, D. H., Investigation of Air-Flow in Two-Stroke Engines, S.M. Thesis, M.I.T., 1948.

Kamins, M. Factors Affecting the Performance of Miniature Two-Stroke Engines. S.M. Thesis, M.I.T., 1949.